Development and application of analytical techniques for the optimization of novel PET tracers used in drug discovery and development.

Development and Application of Analytical Techniques for the Optimization of Novel PET Tracers Used in Drug Discovery and Development

By

Kerry A. Riffel

A Dissertation

Presented to the Graduate and Research Committee

of Lehigh University

in Candidacy for the Degree of Doctor of Philosophy

in

Department of Chemistry

Lehigh University

November 2006

Approved and recommended for acceptance as a dissertation in partial fulfillment of the requirements for the Doctor of Philosophy.

Nov. 27, 2006
Date

December 5, 2006
Accepted Date

Dr. Ned Heindel, Committee Chair

Dr. Natalie Foster

Dr. James Roberts

Dr. Keith Schray

Dr. Donald Burns, Committee Co-Chair

ACKNOWLEDGEMENTS

Support from the department of Imaging Research, Merck Research Laboratories, was in providing facilities, chemicals, and samples used in the studies. Thank you to Dr. Ned Heindel who, as my advisor, provided much support and encouragement. A special appreciation is given to Dr. Donald Burns for assistance in determining what projects could be included in this work.

Positron emission tomography studies require the cooperation of many people to achieve successful results and this work could not have been completed without the following support. Dr. Terence Hamill synthesized tracers for NK_1, mGluR5, and AT_1. He also provided background material for the projects to aid in my understanding of the questions associated with each of the tracers. His support and encouragement was valuable for the completion of this project. Dr. Wenping Li provided synthesis for one of the AT_1 tracers. Dr. Eric Hostetler provided synthesis of Tracer O and Tracer MG as well as assistance with purifying the metabolites of Tracer O. Dr. Stephen Krause, Ms. Christine Ryan, Ms. Liza Gantert, and Ms. Mona Purcell conducted the PET studies described in this research and provided the monkey plasma samples. This research could not have been completed without the support of these individuals.

Finally, appreciation is given to my family for supporting me throughout this experience. They survived classes, qualifiers and finally the writing of this dissertation. I thank them for supporting and encouraging me along the way.

TABLE OF CONTENTS

LIST OF FIGURES

ABSTRACT

Clinical trials routinely include the analysis of plasma samples to determine pharmacokinetic and metabolic properties of new drug entities. However, the determination of drug concentration in the brain is difficult and usually inferred from terminal studies in other species or from sampling of cerebrospinal fluid (CSF). Positron emission tomography (PET) is a minimally invasive imaging procedure widely used for the evaluation of cancer patients. In recent years, PET has gained acceptance as a research tool in drug development. Positron emitting isotopes are used in PET to quantitate regional tissue distribution of radioactivity in living animals and humans. Accurate use of PET requires assessment of metabolism of the tracer to avoid erroneous results from the data. Metabolism of PET tracers can be evaluated in vivo in animal studies and in human subjects by sampling plasma. In vitro metabolism can be used to evaluate and compare metabolism of novel PET tracers in different species. In addition, significant plasma protein binding can prevent a tracer from reaching the target of interest. Thus, PET tracers for the metabotropic glutamate subtype 5 receptor (mGluR5), angiotensin receptor (AT_1), and neurokinin-1 (NK_1) receptor were chosen to conduct method development and optimization of analytical techniques to rapidly analyze radiolabeled metabolites from in vivo plasma samples collected during animal imaging studies and in vitro metabolism studies. Plasma protein binding methods were also optimized for the same tracers. Optimized methods included the use of a monolithic column for HPLC analysis, resulting in significantly reduced sample analysis times. Plasma protein binding measurements were optimized for the use of centrifuge filters by

pre-treating the filters with unlabeled tracer to prevent nonspecific binding of the tracer to the filters. These procedures were used retrospectively to determine whether the studies would have aided the selection of a tracer for clinical studies and/or improved the interpretation of imaging studies. Finally, the methods were applied to two tracers currently in development. The methods and procedures were successful in providing additional support to the evaluation of two novel tracers and are currently used routinely to support tracer development in Imaging Research at Merck Research Laboratories.

1. Introduction

Human clinical studies often include the analysis of plasma samples for the determination of pharmacokinetics and metabolism of a new drug candidate. Procedures for the analysis of plasma samples for drug concentrations are well-developed and relatively straightforward to carry out. High performance liquid chromatography coupled with tandem mass spectrometry (LC-MS/MS) is often used along with liquid-liquid or solid phase extraction to analyze drug concentrations in human plasma or urine samples [1-3]. Determining the level of a drug at a specific target such as a receptor, enzyme, or transporter is more difficult, particularly if the target is in the brain. The blood-brain barrier (BBB) limits the number of compounds that actually enter the brain. Positron emission tomography (PET) offers a means to determine whether a compound has actually reached a target of interest, particularly if the target is in the brain. More importantly, results from a PET study can often be directly correlated to a clinical endpoint.

Positron emission tomography is a powerful, minimally invasive imaging technique for imaging positron-emitting isotopes in the body at a volume of interest. One advantage of PET is that studies performed in animals can also be conducted in humans. Positron emission tomography relies on the availability of positron emitting isotopes such as ^{11}C or ^{18}F to produce a signal that can be captured externally using tomographic methods to produce images [4]. In recent years, PET has gained acceptance as a valuable research tool in drug development. Several types of studies are now commonly used to aid the drug development process. The first type of study involves radio-labeling a drug development compound with a positron emitter, such as ^{11}C or ^{18}F, to evaluate

distribution of the compound to the target and the periphery. These types of studies can be easily scaled from animals to human research subjects and patients [4]. One of the main limitations of this type of study is that not accounting for metabolism can lead to misinterpretation of PET results, since imaging studies alone can not distinguish between labeled tracer and labeled metabolites. A second type of study involves the labeling of a molecule that binds to a receptor and evaluating in vivo competition or target occupancy (target engagement) [4]. The PET signal will decrease with increasing concentration of unlabeled drug compound binding to the same target. Again, metabolism of the PET tracer should be accounted for, or inaccurate results may be obtained if a labeled metabolite reaches the same receptor compartment since labeled metabolites may also lead to changes in apparent non-specific binding of the tracer in a PET scan [4]. Thus, rapid clearance and nonspecifically bound tracer and its metabolites are an important part of the design of a new PET tracer [4]. For example, development of PET tracers selective for the NR2B receptor has been hindered by rapid metabolism of the tracers [5]. Finally, PET can also be used to guide dosing regimens by correlation of receptor occupancy with plasma concentration of the drug [6-8].

Positron emission tomography relies on the detection of radioactivity at a region of interest (ROI or volume of interest, VOI), however it can not be assumed that all radioactivity in the ROI is due to the intact molecule. The signal observed by a PET scan depends on the kinetics of the radiolabeled tracer and the activity in plasma as described by the kinetic model shown in Figure 1 [9].

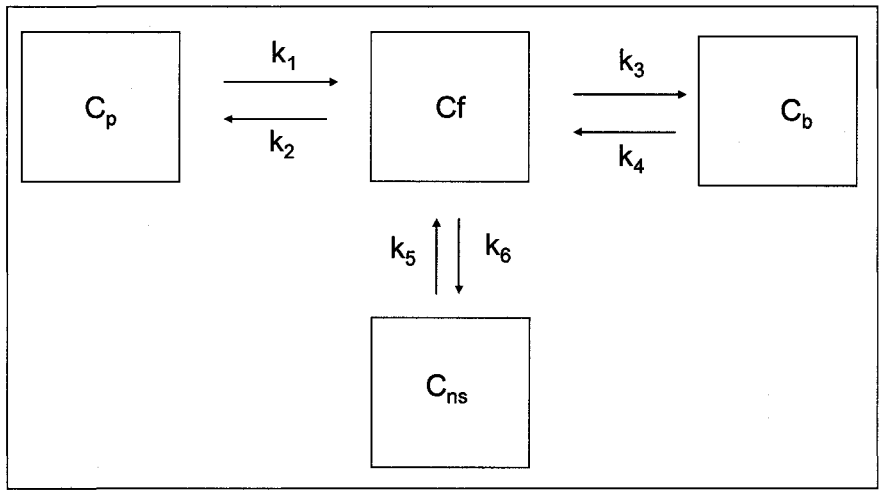

Figure 1. Compartment model for describing the kinetic behavior of a radiolabeled PET tracer in which C_p is the concentration of tracer in plasma, including labeled metabolites; C_f is the free fraction of the tracer; C_{ns} describes non-specific binding of the tracer; and C_b is the tracer that is specifically bound to the receptor of interest; k are the rate constants describing exchange between the compartments [9].

The general model shown in Figure 1 describes the compartments in which the tracer can be located. This model can be evaluated with either an input function or with a reference region, both of which may provide a means to correct for metabolism of the tracer. A reference region is an area with either no known specific binding or a region chosen to indicate baseline binding. The input function involves the use of the following equations that describe model [9]:

Equation 1: $dC_f/dt = k_1Cp(t) - (k_2 + k_3 + k_5)C_f(t) + k_4C_b(t) + k_6C_{ns}(t)$

Equation 2: $dC_b/dt = k_3C_f(t) - k_4C_b(t)$

Equation 3: $dC_{ns}/dt = k_5C_f(t) - k_6C_{ns}(t)$

Equation 4: $C_{tis}(t) = C_f(t) + C_b(t) + C_{ns}(t)$

The concentration at the desired target, C_{tis}, can not be measured in vivo so it is estimated by the following equation [9]:

Equation 5: $C_{PET}(t) = (1 - V_b)C_{tis}(t) + V_bC_{wb}(t)$

The concentration of radioactivity observed from the PET scan at a particular ROI at a given time is C_{PET}, V_b represents the fractional blood volume, and C_{wb} is the radioactivity in whole blood, not corrected for metabolism. Thus, the signal observed by a PET scan depends on the kinetics of the radiolabeled tracer and the activity in blood or plasma, making it necessary to measure activity in blood or plasma samples during the course of a PET scan. The above equation contains two input functions. The input function is the concentration of parent tracer in plasma, and if plasma samples are extracted, metabolite measurements can be included in the modeling process. Labeled metabolites can have different kinetics and should not be included in the input function. The standard model assumes that the labeled metabolites do not enter the tissue, as is often the case in brain studies because metabolites do not cross the blood-brain barrier, but this generalization should be confirmed for a new tracer. The fractional blood volume (V_b) is used to account for intravascular activity. A region of interest defined by a PET scan will include a small fraction of blood vessels which will contribute to the total signal. The intravascular activity is determined by the whole blood concentration and contains metabolites. Both the metabolite-corrected plasma curve and the whole blood curve are required to accurately model the behavior of a PET tracer at a receptor. Given the importance of the metabolite-corrected plasma curve to the model used for the evaluation of a tracer, metabolism of the tracer plays an important role in the successful application of a novel PET tracer [4, 11].

Based on the model described in Figure 1, the free fraction (C_f) of the tracer is available for binding, either specifically (to the target) or non-specifically (to everything

but the target). Determination of the free fraction is thought to be an important parameter in PET kinetic modeling [12], but normally is not included in tracer evaluation. It is possible to estimate C_f from plasma or from a reference tissue. For most drugs, an equilibrium exists between total drug concentration and free fraction of the drug binding to plasma proteins [12]. Plasma protein binding may be useful in the evaluation of a novel PET tracer.

The purpose of the studies conducted for the current work was to develop and apply analytical procedures to improve the analysis of PET imaging studies and/or to optimize the probability of success of novel tracers for applications in clinical trials. Studies for the work reported here focused specifically on the evaluation of animal in vivo metabolism, in vitro metabolism with liver microsomes, and plasma protein binding for several novel PET tracers. High performance liquid chromatography (HPLC) was used as the method of choice for analysis of samples in the metabolism studies. The HPLC was coupled to a sensitive radiochemical detector and a triple quadrupole mass spectrometer, allowing for both the analysis of radiolabeled metabolites and the partial identification of metabolites when needed. Various HPLC conditions were evaluated, including the use of a monolithic column which has the advantage of a high flow rate and fast analysis time. Centrifuge filters were chosen for the determination of plasma protein binding because they were the most rapid method available. Centrifuge filters may not be as accurate as more traditional dialysis methods, however the half-lives of the tracers prevent the use of long dialysis experiments [13]. All metabolism and protein binding studies were performed at tracer level, with no addition of cold compound in order to mimic in vivo

studies as closely as possible. Given the generally high specific activity of PET tracers, there is very little mass of the compound present in imaging studies.

2. Background

The application of a novel PET tracer may be limited by rapid metabolism and high plasma protein binding of the tracer. The short half-lives of PET tracers (20 min for ^{11}C and 109 min for ^{18}F) coupled with extensive metabolism often lead to low amounts of radioactivity in plasma samples at later time points during a typical PET study [4]. Metabolic stability of novel PET tracers has been evaluated both from in vivo animal studies and from in vitro microsome studies. The short half-lives of PET tracers require analytical procedures be rapid and sensitive. Current methodology includes analysis by HPLC with a radiochemical detector or HPLC with fraction collection followed by gamma counting of the fractions. Limitations of current methodology include long run times, leading to poor sensitivity, or the inability to analyze multiple samples prior to radiochemical decay. In the case of fraction collection, the metabolites may not be separated from each other and there is often no confirmation of separation of metabolites from parent tracer, which can lead to erroneous correction for the metabolism of the tracer. Fraction collection is not often coupled with a method that allows for metabolite identification.

Metabolic stability of a novel PET tracer has been evaluated both from in vivo animal studies and from in vitro microsome studies. Lee et al. [14] employed in vitro metabolism to predict metabolism in vivo of two [^{18}F]-labeled acetylcholinesterase inhibitors. Study results indicated that the presence of in vivo metabolites could be predicted from in vitro

metabolism studies. However, rates of metabolism in vitro and in vivo could not be directly compared. Metabolic stability of two ^{18}F-labeled phenylpiperazine radiotracers was investigated in vitro using mouse liver S9 fractions [15]. The results were compared to in vivo metabolism using mouse blood and bone and to in vitro metabolism obtained using liver microsomes. Based on the study results, both liver S9 fractions and liver microsomes produced the same metabolites as in vivo metabolism for the tracers that were studied. The metabolic stability of flumazenil in rat liver microsomes was investigated using high flow rate extraction coupled to capillary liquid chromatography-mass spectrometry [16]. The validated procedures were useful for evaluating the metabolic stability of flumazenil. In addition, the authors illustrated the use of [^{11}C]flumazenil during development of a new drug candidate. In vitro metabolism of labeled and unlabeled [^{18}F]fluoroethylflumazenil was evaluated using HPLC and tandem mass spectrometry [17]. Several metabolites were identified in rat and human microsome samples. The unlabeled PET tracer WAY-100635 and two of its analogs were evaluated for metabolic stability using LC-MS/MS [18]. The advantage of LC-MS/MS was that the unlabeled tracers could be evaluated at low nM concentration levels which are typical in PET studies. However, these studies were not used to directly correlate radiolabeled peaks with LC-MS/MS peaks.

Metabolism of PET tracers in plasma samples has been evaluated using several techniques. An HPLC column-switching technique was reported by Hilton et al. [19] for the analysis of 4 mL plasma samples for metabolites of [^{11}C]-labeled PET tracers. The samples were treated with 8M urea to disrupt protein binding and all but the most polar metabolites were detected. Methods have been described for the analysis of

[^{11}C]NNC112, [^{11}C]NS 2214, [^{11}C]PK1195, and [^{11}C]raclopride in plasma obtained from arterial blood of living minipigs [20]. In this case, the plasma samples were deproteinated with acetonitrile and analyzed by HPLC with a radiochemical detector. Using kinetic analysis, the apparent metabolism of the tracers in plasma was quantified. Zea-Ponce et al. [21] describe an acetonitrile protein precipitation and HPLC procedure for measuring [^{123}I]IBZM in human plasma with 95% recovery. Online SPE-HPLC was utilized for the analysis of [(*R*)-[^{11}C]PK-11195 in human plasma with sample recoveries of more than 98% [22]. The online technique was compared to samples analyzed using offline methods. For plasma samples taken at later time points, the offline method provided the most reproducible results. Liquid-liquid and solid phase extraction methods were used for the determination of [^{18}F]FCWAY and [^{18}F]FP-TZTP in human plasma [19]. The methods were found to be faster and easier to apply, with results comparable to those obtained by HPLC or thin layer chromatography (TLC). L-[methyl-^{11}C]methionine and its metabolites were analyzed in human plasma by an automated solid phase extraction procedure with HPLC for analysis with greater than 95% recovery [24]. Supercritical fluid extraction was employed for the analysis of *O*-[2-^{11}C]acetyl-L-carnitine and *N*-[^{11}C]methylpiperidyl benzilate in the kidneys and brains extracted from rats after injection of the tracers [25]. After supercritical fluid extraction, the labeled metabolites were analyzed by HPLC or LC/MS.

Along with metabolism, plasma protein binding may also be a benefit in determining whether a PET tracer will provide valuable results in human studies. An equilibrium exists between total drug concentration and free drug concentration in plasma and tissues and for most drugs, a specific fraction of the drug is bound to plasma proteins. Drugs

bind to numerous plasma proteins, however the two major drug-binding proteins are albumin and alpha-1-acid glycoprotein (AAG). Generally, the unbound fractions of drug are available to tissues for pharmacological activity [26]. However, in the case of brain-penetrable drugs, the blood-brain barrier must also be considered. Plasma protein binding has been studied in an attempt to explain differences in brain penetration of drugs. Based on studies with several antihistamines in rats, a balance of passive membrane permeability, P-gp-mediated efflux, and high plasma protein binding all influence the in vivo brain distribution of antihistamines [27]. Plasma protein binding had a dramatic effect on the brain uptake of three non-steroidal anti-inflammatory drugs (NSAIDs), where the plasma free fraction in vivo of the three NSAIDs was reduced by >90% [28].

Plasma protein binding of several PET tracers has been evaluated as part of their development. Wilson et al. [12] showed that ultrafiltration could be utilized to determine the plasma protein binding, or free fraction, for a PET tracer for imaging dopamine receptors. The free fraction in human plasma was 41% and thought to be adequate for accurate measurements in PET studies with human subjects. The correlation between plasma protein binding and ligand fraction for [^{18}F]fluorocarazolol was used to correct input functions of compartment models to evaluate the effect of protein binding on PET data [29]. Protein binding for [^{11}C]methoxynorchloroprogabidic acid ([^{11}C])MNPGA), a radioligand for the GABA receptor, was found to be 89% [30]. Interestingly, plasma protein binding for the nonlabeled drug was >95%. When taking the plasma free fraction into account, the distribution volume was thought to be suitable for transfer of the radioligand into the brain. However, human PET studies with the same tracer resulted in low uptake of the tracer in the brain. [O-methyl-^{11}C]RS-15385-197 exhibited very low

brain uptake in human PET studies after successful imaging studies in rat [31]. Retrospective plasma protein binding studies resulted in higher protein binding of the tracer in human plasma compared to rat plasma. The authors suggested that the tracer may have had a higher affinity for plasma proteins than the receptor, limiting the transport of the ligand into the brain. Mankoff et al. [32] evaluated the plasma protein binding of [^{18}F]-16α-fluoroestradiol (FES) in human plasma using size exclusion chromatography. High plasma protein binding was observed for the tracer. During the evaluation of [^{11}C](R)-(-)-RWAY, pretreatment with tariquidar, a potent inhibitor of P-gP, resulted in increased brain uptake of [^{11}C](R)-(-)-RWAY by 1.5–fold and the plasma free fraction by 1.8-fold. The effect on brain uptake was thought to be due to the decrease in radioligand binding to plasma proteins [33].

3. Experimental Objectives

The current research used plasma protein binding as one consideration of the possible success or failure of PET tracers in clinical studies. The studies presented here also evaluated animal in vivo and in vitro metabolism with liver microsomes and plasma protein binding for several novel PET tracers to determine whether results from these experiments could contribute to the prediction of success of a PET tracer in human studies. Methods and procedures were optimized for all analyses using several previously reported PET tracers. The optimized methods and procedures were then applied to tracers currently in development. The results of the incubations with monkey, dog and human liver microsomes were compared to predict whether metabolism in human subjects will be too rapid for a successful PET study in human subjects. Although prediction of human

metabolism from microsomal metabolism data is difficult, the results could serve as a guide as to whether further development of the tracer is warranted [34]. PET tracers for the metabotropic glutamate subtype 5 receptor (mGluR5), angiotensin receptor (AT_1), and neurokinin receptors (NK_1) were evaluated. Each PET tracer has been evaluated in animal PET studies, however, the mGluR5 tracer has not yet been evaluated in human studies [35]. The AT_1 PET tracer successfully imaged the AT_1 receptors in vivo in dog studies but was not successful in human studies [36]. One of the NK_1 tracers evaluated has been successfully applied in human studies [37-40]. Finally, data are presented from several PET tracers still in development where in vitro metabolism and plasma protein binding added further support for the continuation of a program or explanation for inconclusive results from animal PET studies.

Several PET tracers for the mGluR5 receptor have been reported. The mGluR5 receptor is distributed throughout the CNS and has been suggested to be a potential target for a number of disorders, including Parkinson's disease, pain, anxiety, depression and addiction [35]. The synthesis and radiolabeling of three PET ligands (2-[^{11}C]methyl-6-(2-phenylethynyl)pyridine ([^{11}C]MPEP); 2-(2-(3-[^{11}C]methoxyphenyl)ethynyl)pyridine ([^{11}C]Methoxy-MPEP); and 2-(2-(5-[^{11}C]methoxypyridin-3-yl)ethynyl)pyridine ([^{11}C]Methoxy-PEPy)) for the mGluR5 receptor were used in microPET studies in rats [41]. Rapid metabolism was observed in the rat studies, however none of the metabolites were lipophilic based on HPLC results. Binding of all three ligands was very fast, thus rapid metabolism may not be an issue. All three tracers were considered suitable for further development as PET ligands for mGluR5 receptors. Increased uptake of [^{11}C]methoxyMPEP was observed in rat PET studies when coinjected with unlabeled

methoxyMPEP [42]. Musachio et al. [43] found rapid uptake and washout in the brain, as well as uniform distribution, in rats and monkeys with [^{11}C]methoxyMPEP. There was no significant difference in radioactivity uptake in different regions of the brain between control rats and those co-injected with methoxyMPEP for [^{11}C]-2-methyl-6-(3-fluorophenylethynyl-pyridine ([^{11}C]M-FPEP) [44]. [^{11}C]MethoxyMTEP was shown to enter the brain of rhesus monkeys and produce a short-lived specific signal [45, 46]. Most recently, Ametamey et al. [47] reported the synthesis and evaluation of [^{11}C]ABP688 (3-(6-methyl-pyridin-2-ylethynyl)-cyclohex-2-enone-O-(11)C-methyl-oxime) as a probe for the mGluR5 receptor. MicroPET blocking studies were performed in rats, revealing up to 80% specific binding in rat brain [47]. The tracer was found to be selective for imaging mGluR5 in vivo in rodents. Structures of previously reported PET tracers for imaging the mGluR5 receptors are shown in Figure 2.

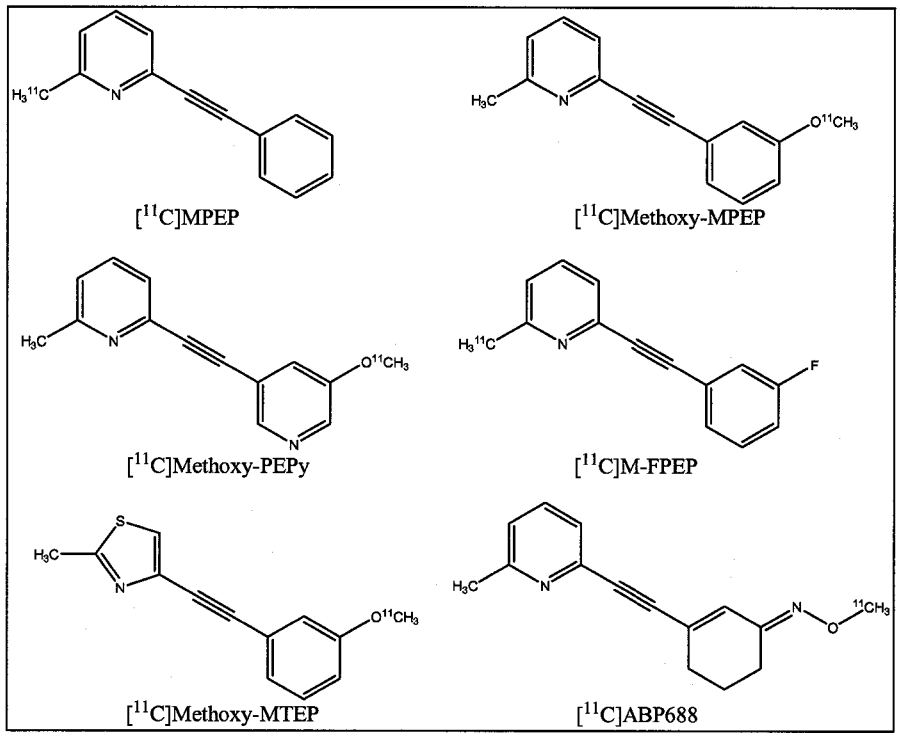

Figure 2. Structures of previously reported PET tracers for imaging mGluR5 receptors [41, 42, 44, 47].

Hamill et al. [35] reported the first successful monkey imaging studies of the mGluR5 receptor with three PET tracers (Figure 3): [^{11}C]3-methyl-5-[(2-methyl-1,3-thiazol-4-yl)ethynyl]benzonitrile ([^{11}C]M-MTEB), [^{18}F]3-fluoro-5-[(2-methyl-1,3-thiazol-4-yl-ethynyl)benzonitrile ([^{18}F]F-MTEB), and [^{18}F]3-fluoro-5-[(pyridine-3-yl)ethynyl]benzonitrile ([^{18}F]F-PEB). Large, long-lived specific signals were observed during separate imaging studies with all three tracers. Equilibrium was reached in a reasonable time to conduct a PET imaging study.

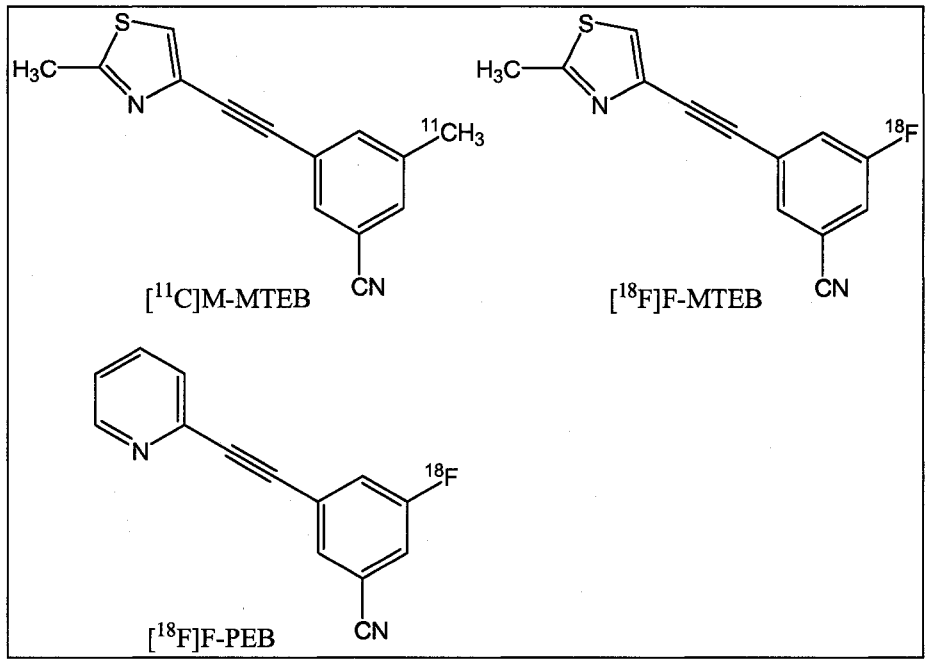

Figure 3. Structures of mGluR5 PET tracers reported by Hamill et al. [35]. [^{18}F]F-PEB is the PET tracer evaluated in the studies described herein.

Experiments for the current study focused on in vivo metabolism in rhesus monkeys as well as in vitro metabolism in rhesus monkey and human liver microsomes for [^{18}F]F-PEB to determine whether metabolism may predict the success of the tracer in human studies. Plasma protein binding in rhesus monkey and human were also evaluated.

In addition to evaluating metabolism of [^{18}F]F-PEB, methods of analysis were also evaluated. All samples were analyzed for the radiolabeled tracer using liquid chromatography and a radiochemical detector. Two different HPLC methods of analysis were evaluated: a traditional HPLC column was compared to the use of a monolithic column to increase the speed of analysis. The main advantages of using the monolithic column is that plasma can be directly injected onto the column and high flow rates can be used, decreasing analysis time [48, 49].

Angiotensin II (Ang II) plays a role in the regulation of cardiovascular function. Ang II receptors exist in two forms, with AT_1 responsible for known pressor effects of Ang II. The development of an AT_1 selective radiotracer for use in PET imaging would be useful in aiding the development of orally active antihypertensive agents [50]. The first reported PET tracer for imaging ANG II receptors was [^{11}C]L-159,884 ([^{11}C]*N*-[[4'[(2-ethyl-5,7-dimethyl-3H-imidazo[4,5-b]pyridine-3-yl)methyl][1,1'-biphenyl]-2-yl]sulfonyl]-4-methoxybenzamide, Figure 5) [50]. This tracer was successful for PET imaging in mice and canine studies [51-53], however rapid metabolism was observed in initial studies in human subjects (unpublished data). Thus, the compound appears to be unsuitable as a tracer for use in human studies. More recently, [^{11}C]L-159,884 was used in PET studies in beagle dogs to evaluate the estrogen regulation of adrenal and renal angiotensin (AT_1) receptor [54]. Furthermore, Zober et al. [55] reported the use of [^{11}C]KR31173 (Figure 4) in PET imaging studies in baboons and dogs. Results were compared to those obtained from imaging studies with [^{11}C]L-159,884 and showed that [^{11}C]KR31173 possessed lower protein binding. There was higher uptake and specific binding of [^{11}C]KR31173 in baboon kidney when compared to [^{11}C]L-159,884 [55].

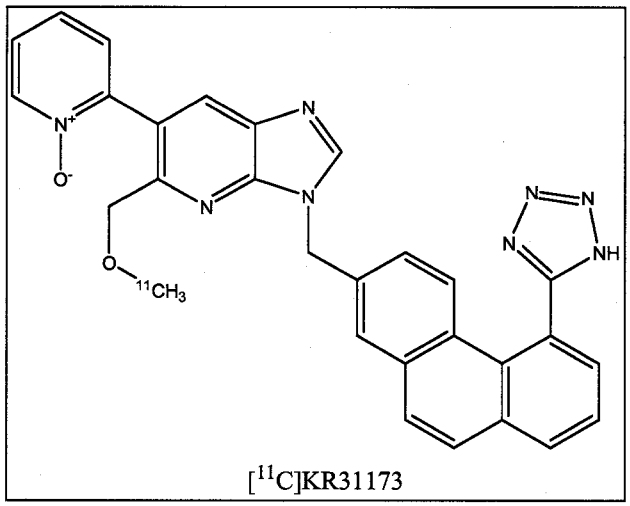

Figure 4. Structure of [^{11}C]KR31173, a PET tracer for imaging AT1 receptors reported in the literature [55].

For the current work, studies were performed with [^{11}C]L-159,884 and [^{18}F]*N*-[[4'[(2-ethyl-5,7-dimethyl-3H-imidazol[4,5-b]pyridine-3-yl)methyl][1,1'biphenyl]-2-yl]sulfonyl]-4-fluorodideuteromethoxybenzamide ([^{18}F]FMe-L-159,884-d_2, Figure 5) to determine whether in vitro techniques could have been used to predict the failure of the tracer in human studies and to compare the results obtained from the ^{18}F-labeled compound. Protein binding of each tracer was determined in dog, monkey and human plasma. In vitro metabolism was evaluated in the same species using liver microsomes. The results from the plasma protein binding and in vitro metabolism studies were evaluated to determine whether these techniques would have been applicable in predicting the failure of the [^{11}C]-labeled tracer or the success of the [^{18}F]-labeled tracer in human studies.

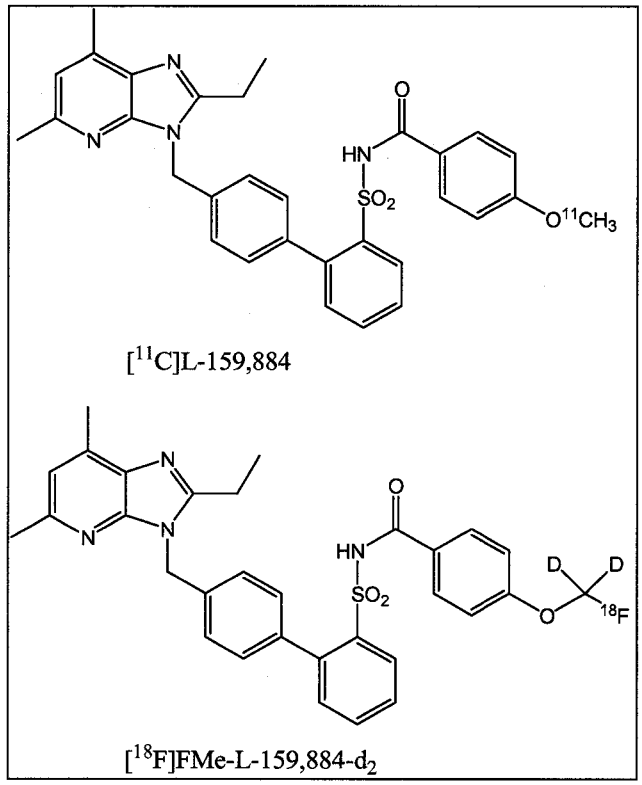

Figure 5. Structures of AT_1 PET tracers evaluated in these studies.

Positron emission tomography has been used to successfully image the substance P receptors in the human brain [37]. Substance P (SP) is an undecapeptide that is widely distributed in the central nervous system and appears to be to be found along with other neurotransmitters, usually serotonin. There are three neurokinin receptor subtypes (NK_1, NK_2 and NK_3); NK_1 is the receptor for SP. The NK_1 receptors have been implicated in regulation of various diseases such as depression, pain, anxiety, and emesis [56].

Several structurally similar NK_1 antagonists have been developed for use as potential PET tracers. One compound, CP-96,345 was a high affinity antagonist of the NK_1 receptor. Very little [^{11}C]CP-96,345 (Figure 6) observed in any area of the brain after imaging studies in guinea pigs.. As a result, this tracer was later found not to be suitable

for use as an in vivo marker of substance P receptors in the brain [57]. [^{11}C]CP-99,994 (Figure 6) was found to have better brain penetration than CP-96,345. Based on imaging study results, [^{11}C]CP-99,994 could be an excellent tracer for pharmacokinetic studies of CP-99,994 in both animals and humans by PET [58]. Two other high affinity and selective NK_1 receptor antagonists, GR-203040 and GR-205171 (Figure 6), were labeled with ^{11}C and used in experiments with rhesus monkeys [8]. Overall, [^{11}C]GR-203040 (Figure 6) showed less favorable properties for the *in vivo* characterization of NK_1 receptors. The use of [^{11}C]GR-205171 (Figure 6) is also limited because it does not reach equilibrium during typical PET scan times which confounds determination of receptor concentration. However, imaging studies with [^{11}C]GR-205171 were conducted to evaluate how the activity in the NK_1 receptor system was affected by fear provocation in human subjects with a specific phobia by PET [59]. Brain uptake and distribution of *N*-[^{11}C]methyl CP-643,051 (Figure 6) in the pig brain was investigated by PET [60]. The tracer was found to exhibit low specific binding so was not a suitable PET ligand for the NK_1 receptor system. Finally, Gao et al. [61] reported the synthesis and PET imaging in rats of [^{11}C]BMP (Figure 6) and [^{11}C]BME (Figure 6). Based on results from blocking studies, the presence of both tracers in the rat brain was due to nonspecific processes, thus the tracers would not be adequate for imaging NK_1 receptors in the brain.

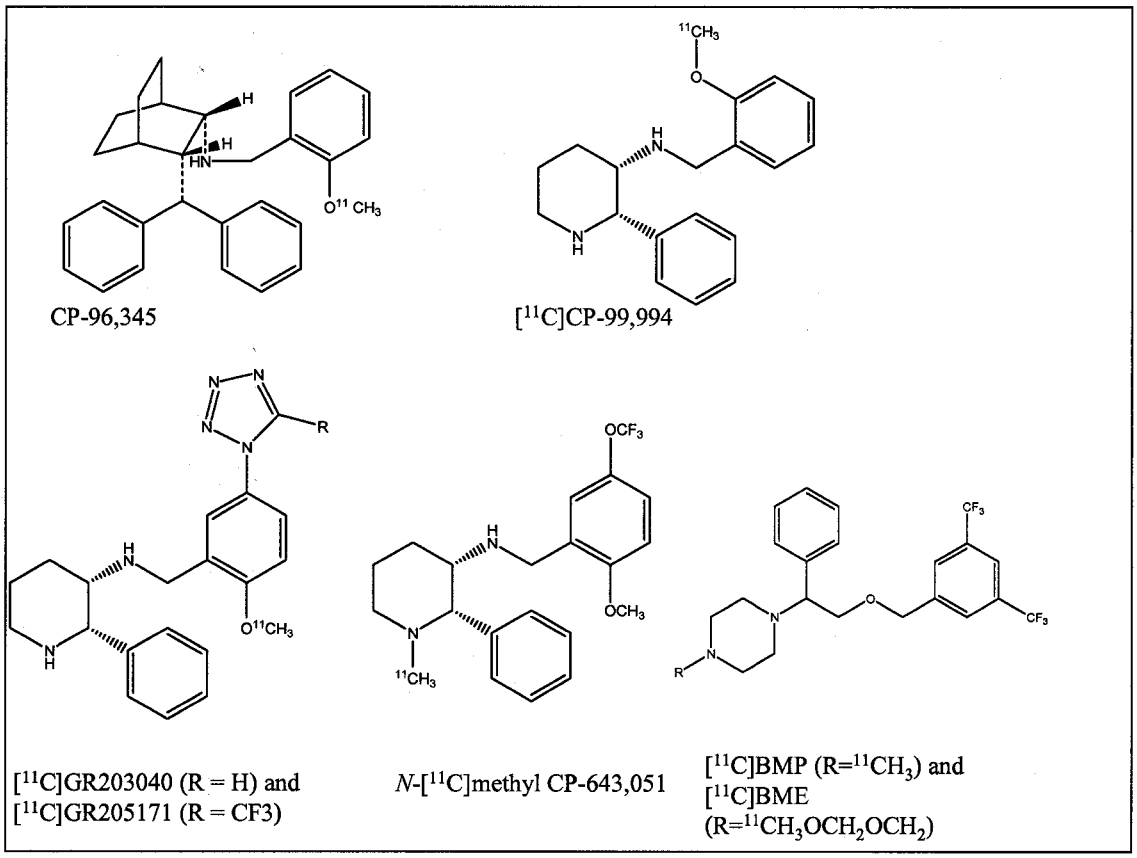

Figure 6. Structures of previously reported PET tracers for the NK_1 receptor [8, 57, 58, 60, 61].

The synthesis and characterization of an ^{18}F-labeled NK_1 receptor antagonist with high affinity for the NK_1 receptor has been reported [62]. Based on studies in guinea pigs, [^{18}F]SPA-RQ ([^{18}F][2-fluoromethoxy-5-(5-trifluoromethyl-tetrazol-1-yl)-benzyl]-([2S,3S])-2-phenyl-piperidin-3-yl)-amine, Figure 7) was thought to be a suitable tracer for PET studies in monkeys and humans. The use of [^{18}F]SPA-RQ in human PET imaging studies has been reported. Bergstrom et al. [38] report the use of [^{18}F]SPA-RQ and PET imaging to study NK_1 receptor occupancy of aprepitant to guide dose selection in human clinical studies. Aprepitant is a highly selective substance P antagonist that is used in the treatment of chemotherapy-induced and post-operative nausea and vomiting.

Positron emission tomography studies were performed in a human clinical study on the last day of a 14-day dosing regimen. The study concluded that PET imaging with [^{18}F]SPA-RQ allows for the brain receptor occupancy of aprepitant to be determined from aprepitant plasma concentrations. Additionally, [^{18}F]SPA-RQ can be used to guide dose selection for clinical trials of newly developed NK_1 receptor antagonists. [^{18}F]SPA-RQ was also used to show the lack of efficacy of aprepitant for the treatment of depression [63]. Results from five clinical trials and over 2500 patients who received chronic 80 mg and 160 mg doses of aprepitant were included. Based on traditional depression tests, there was no difference in the anti-depressive effect between aprepitant and placebo. Imaging studies were performed in 18 subjects who received the same dosing regimen. Receptor occupancy was sufficient for a biological response as observed by the PET studies. The authors concluded that NK_1 receptor antagonism for the treatment of depression is not supported [63]. Imaging studies with [^{18}F]SPA-RQ were also employed to quantify the NK_1 receptors in the human brain using PET [39]. Distribution of NK_1 receptors in vivo in the human brain was observed by PET and the receptors were found to be distributed throughout the brain, with the highest density in the striatum and visual cortex. Imaging studies with [^{18}F]SPA-RQ was also used to show that gender and age affect NK_1 receptors in the human brain [40].

Early in the development of [^{18}F]SPA-RQ, nonspecific labeling in the bone was observed from PET imaging studies in monkeys as viewed by uptake of tracer in the skull (unpublished results). This is a strong indication of dealkylation of the tracer leading to the presence of [^{18}F]F-, as bone tends to be the capture locus for free fluoride in vivo. In vitro metabolism studies performed with unlabeled SPA-RQ at concentrations of 1 μM

and 10 μM showed that the major metabolite was due to O-dealkylation resulting in the loss of the fluoromethyl group leading to the phenol metabolite. Although the mechanism was not determined, it is possible fluoroacetadlehyde or fluoroacetic acid were formed prior to the loss of F- [64]. As a result, both deutero-fluoromethoxy ([^{18}F][2-fluorodideuteromethoxy-5-(5-trifluoromethyl-tetrazol-1-yl)-benzyl]-([2S,3S]-2-phenyl-piperidin-3-yl)-amine, [^{18}F]SPARQ-d_2, Figure 7) and fluoroethoxy ([^{18}F][2-fluoroethoxy-5-(5-trifluoromethyl-tetrazol-1-yl)-benzyl]-([2S,3S]-2-phenyl-piperidin-3-yl)amine, [^{18}F]FESPA-RQ, Figure 7) analogs were synthesized with the expectation that these would be less prone to metabolic loss of fluorine.

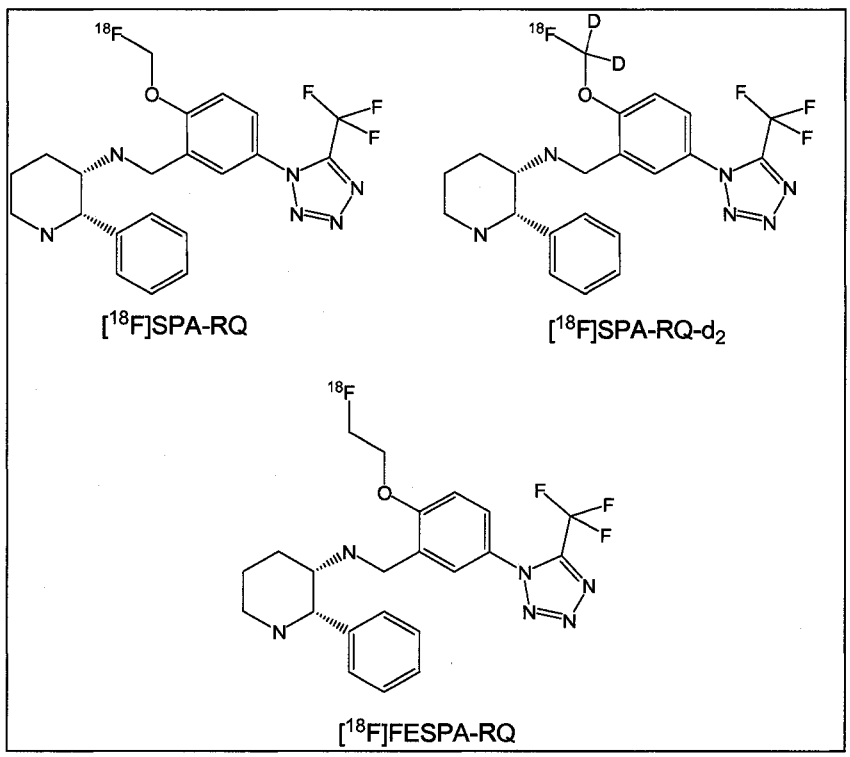

Figure 7. Structures of NK_1 PET tracers to be evaluated in these studies.

The use of deuterium in a molecule does not alter the pharmacological activity or distribution of a particular molecule. However, deuteration can be expected to reduce the rate of defluorination of the fluoromethyl group due to the isotope effect [65]. When the C-H bond is the rate-limiting step in the metabolism of parent tracer, the tracer would be expected to be more stable with a C-D bond because it is a more difficult bond to break, thus producing a metabolic switch [65, 66]. However, kinetic issues may prevent the change in metabolism. Traditional isotope effect studies have been conducted in mechanistic studies to identify the exact carbon-hydrogen bond responsible for a chemical or biophysical transformation. However, several successful cases of deuterated PET tracers employed to limit metabolism of the tracer have been reported. Comparison of [^{11}C]L-deprenyl and [^{11}C]L-deprenyl-α,α-$^{2}H_2$ in baboon plasma showed similar metabolism for the two tracers in plasma [67]. However, in mouse brain, deuterium substitution significantly reduced the amount of radioactivity bound to protein [67]. Fowler et al. [68] later reported the deuteration of [^{11}C]L-deprenyl and found that the total ^{11}C concentration in plasma was higher for the deuterated tracer. Furthermore, the authors showed that there was a deuterium isotope effect for [^{11}C]L-deprenyl trapping in the brain. Staley et al. [65] report the synthesis of [^{18}F]deuteroaltanserin as a means to prevent the metabolism observed in human studies with [^{18}F]altanserin. Imaging studies with [^{18}F]altanserin in human subjects have been limited by the presence of radiolabeled metabolites that cross the blood-brain barrier. [^{18}F]deuteroaltanserin was more slowly metabolized in human studies. Both [^{18}F]deuteroaltanserin and [^{18}F]altanserin were evaluated in two baboons and found that there was no significant difference between the two tracers in either baboon. The authors suggested a possible species difference in

metabolism to explain the difference in study results[65]. Ding et al. [69] reported the comparison of 6-[^{18}F]fluorodopa (6-[^{18}F]FDA) and deuterated 6-[^{18}F]fluorodopa (6-[^{18}F]FDA-α,α-D2). A large decrease in clearance for 6-[^{18}F]FDA-α,α-D2 compared to 6-[^{18}F]FDA was observed. The studies were used to demonstrate that deuterium substitution can protect a radiotracer from metabolism in vivo. An [^{18}F]-labeled PET tracer and its deuterated analog for the peripheral benzodiazepine receptor (PBR) were evaluated in mouse plasma and brain [70]. No difference in the metabolism between the two tracers was observed in plasma, but in the brain the deuterated analog was metabolized much slower. The deuterated analog did not show a decreased level of activity in monkey skull as evaluated by PET. Thus, a species difference in the metabolism of the tracers between mice and primates may exist. Lin et al. [71] report the synthesis and biodistribution of ^{18}F-labeled raboxetine analogs, including both a fluoroethoxy ([^{18}F]FRB) and tetradeuterated ([^{18}F]FRB-D_4) analog. Biodistribution studies in mice achieved similar results with both tracers and [^{18}F]FRB-D_4 exhibited relatively faster blood clearance than [^{18}F]FRB with no significant in vivo defluorination. In addition, [^{18}F]FRB-D_4 may be a potentially useful radioligand for imaging the norepinephrine transporter in vivo by PET based on PET studies in baboon brain [71].

Several studies were conducted to compare the brain uptake and metabolism in plasma samples of fluoroethyl and fluoromethyl analogs of the same PET tracer. Zhang et al. [72] compared uptake in mouse brain of fluoroethyl and fluoromethyl analogs of PET tracers designed for imaging of peripheral benzodiazepine receptor (PBR). Uptake in bone with the fluoromethyl analog but little to no uptake in bone for the fluoroethyl analog were observed by PET imaging studies. In addition, metabolism was evaluated in

mouse plasma and [^{18}F]F- was confirmed by ion exchange chromatography after treatment with the fluoromethyl analog. There was no [^{18}F]F- present in either mouse or monkey plasma after treatment with the fluoroethyl analog. Tsukada et al. [73] compared the tumor uptake of [^{18}F]fluoromethyl tyrosine ([^{18}F]FMT), [^{18}F]fluoroethyl tyrosine ([^{18}F]FET), and [^{18}F]fluoropropyl tyrosine ([^{18}F]FPT). Metabolism of all the tracers was evaluated in plasma samples after injection of the tracers in mice. There was little difference in metabolism between the three tracers and the compounds were all found to be generally stable.

During optimization of [^{18}F]SPA-RQ as a PET tracer for imaging NK_1 receptors in vivo, additional PET imaging studies were performed in the same monkey with all three NK_1 tracer. Generally less bone uptake was observed with [^{18}F]FESPA-RQ than with [^{18}F]SPA-RQ with overall higher brain uptake for [^{18}F]SPA-RQ. The differences between [^{18}F]SPA-RQ-d_2 and [^{18}F]FESPA-RQ were similar with overall brain uptake higher for [^{18}F]SPA-RQ-d_2 (unpublished data). Additionally, in vivo metabolism of [^{18}F]SPA-RQ and [^{18}F]SPA-RQ-d_2 was evaluated in rhesus monkey plasma by thin layer chromatography (TLC). Slightly less metabolism was observed for [^{18}F]SPA-RQ-d_2 at 120 min post-injection, however TLC was not capable of determining whether the more polar labeled metabolites were due to the presence of [^{18}F]F-, which would result in the apparent bone uptake in the PET results. Based on unpublished results of in vitro metabolism studies of SPA-RQ (10 μM), a species difference may exist for the metabolism of the tracer between monkey and human. In vitro metabolism was much slower in human liver microsomes than in monkey liver microsomes. Based on these

results and the higher uptake of [^{18}F]SPA-RQ in the brain of monkeys, [^{18}F]SPA-RQ was chosen for human studies.

In this dissertation, in vitro metabolism of [^{18}F]SPA-RQ, [^{18}F]SPA-RQ-d_2, and [^{18}F]FESPA-RQ (Figure 7), was evaluated in rhesus monkey and human liver microsomes. In vivo metabolism of the tracers was also compared in rhesus monkey plasma. In all metabolism studies, chromatograms were evaluated for the presence of [^{18}F]F-, commonly present as a radioactive peak at the HPLC column dead volume, to determine whether these methods would have been useful in guiding the selection of the PET tracer prior to human studies. Protein binding of the same tracers was also evaluated in rhesus monkey and human plasma to determine whether any significant differences occur between the species.

In summary, the mGluR5, AT_1, and NK_1 PET tracers were used to develop and optimize methods for the determination of in vivo and in vitro metabolism and plasma protein binding. This information serves as a retrospective means for determining whether a tracer will be successful in human clinical studies. The methods developed herein were then applied to the analysis of two novel tracers currently in development.

In the first case, in vitro metabolism was used to prepare labeled metabolites of a novel [^{18}F]-labeled PET tracer ([^{18}F]Tracer O) being developed in support of an ongoing clinical research program. Several labeled metabolites of [^{18}F]Tracer O were observed in rhesus monkey plasma samples. The metabolites eluted closely to the parent tracer on the HPLC chromatogram. Given the similarity in polarity of the labeled metabolites to the parent tracer, it is possible that the labeled metabolites could potentially cross the blood-brain barrier and confound the PET signal. There is no reference region available for

modeling the PET data for [^{18}F]Tracer O. Thus, any significant differences in metabolism could lead to an increase in the nonspecific signal in the PET scan. The metabolites were the result of a hydroxylation with the additional OH being placed in one of several locations on a cyclohexyl ring. Due to the large number of possible metabolites, synthesis of all the potential metabolites is not possible, thus the parent tracer was synthesized and incubated with rhesus monkey liver microsomes to make enough labeled metabolites to inject in a rhesus monkey for a PET imaging study. The labeled metabolites were evaluated for uptake in the brain as well as evaluated in vivo in plasma during the course of the PET scan.

In the second case, [^{18}F]Tracer MG binds to a specific receptor in the brain and was evaluated in PET studies in rhesus monkeys in support of drug development activities. Based on baseline scans in several monkey PET imaging studies, good uptake in the brain of [^{18}F]Tracer MG was observed. In addition, reasonable metabolism of the tracer was observed as evaluated in monkey plasma by HPLC with a radiochemical detector. The tracer was evaluated in PET imaging receptor occupancy studies to support the development of several drug candidates in the program. Blocking studies were performed by administering a bolus+infusion of a drug compound that is suspected to bind to the receptor of interest, followed by administration of the tracer. Ordinarily, blocking studies should lead to less uptake of the tracer at the region of interest than in a baseline study of tracer alone because uptake of the tracer at the receptor is blocked by the drug compound. However, in the case of [^{18}F]Tracer MG, increased receptor binding of the tracer in the presence of the blocking drug (BD) was observed from the PET studies. In vivo metabolism and plasma protein binding were both investigated as possible explanations

for the results obtained from the PET studies. In vivo metabolism of the tracer was evaluated in two monkeys both with and without administration of the blocking drug. For plasma protein binding, plasma was obtained from the monkeys being studied prior to administration of the blocking drug and again at the end of drug infusion. The plasma was then treated with the tracer and incubated before using centrifuge filters to separate tracer in total plasma (containing plasma proteins) from tracer in free plasma. An explanation of this unexpected result will be discussed later herein.

This dissertation also demonstrates that HPLC coupled with radiodetection and LC-MS/MS can be used along with in vitro and in vivo metabolism to aid in the successful development of novel PET tracers for use in imaging human subjects. Furthermore, plasma protein binding can be used to guide development of novel PET tracers.

4. Experimental Materials and Procedures

4.1 Tracer Preparation

All tracers were prepared by radiochemists in Imaging Research at Merck Research Laboratories (West Point, PA) or, in the case of a majority of the NK_1 tracers, by staff at Siemens Biomedical Solutions (North Wales, PA).

mGluR5 ([^{18}F]F-PEB). Synthesis of [^{18}F]F-PEB was performed as needed according to the procedures described by Hamill et al. [35]. Specific activities of the tracers were 685 – 6398 Ci/mmol with >98% purity (n = 14).

NK_1 ([^{18}F]SPA-RQ, [^{18}F]SPA-RQ-d_2 and [^{18}F]FESPA-RQ). Synthesis of [^{18}F]SPA-RQ was performed following the procedures described by Solin et al. [62].

The following procedures were utilized as needed for the preparation of [^{18}F]SPA-RQ-d_2. The resin containing the [^{18}F]F^- was eluted with 1.5 mL of a solution of 80:20 MeCN:oxalate solution [0.05 mL of (200 mg $K_2C_2O_4$/3 mg K_2CO_3/5 mL H_2O) + 0.25 mL H_2O + 1.2 mL MeCN] and transferred to the reaction vessel. A solution (0.2mL) of Kryptofix222 (36 mg/mL MeCN) was added and the mixture was heated to 95 °C under vacuum and argon flow to dryness. Additional aliquots of MeCN (3 x 0.7 mL) were used to further dry the [^{18}F]F^-. A solution of CD_2Br_2 (0.05 mL) in MeCN (1 mL) was added and the mixture was heated at 95 °C. Argon flow was used to distill the [^{18}F]FCD_2Br into a vial at 0°C that contains 0.3 mg of (2S,3S)-1-t-butoxycarbonyl-2-phenyl-3-[2-hydroxy-5-(5'-trifluoro-methyltetrazo-1-yl)phenylmethylene-amino]-piperidine) in 0.2 mL of DMF and ~ 1-2mg of cesium carbonate. After the amount of radioactivity in the reaction vial peaked, the distillation was stopped and the reaction vial was heated at 100°C for 7 minutes. The DMF was removed over five minutes using an argon flow at 100°C and 0.1 mL of TFA was then added and allowed to sit at 100°C for 30 seconds. The reaction mixture was diluted with 0.2 mL of ethanol and 0.6 mL of H_2O and purified by preparative HPLC [Waters C18 μBondapak, 7.8 x 300 mm, 3 mL/minute, 20 minute linear gradient 20:80 to 90:10 acetonitrile:H_2O (95:5:0.1 H_2O:MeCN:TFA)]. The product elutes at ~ 12 minutes. Specific activities of the tracers were 510-4007 Ci/mmol with >98% purity (n = 9).

The following procedures were used for the preparation of [^{18}F]FESPA-RQ. The [^{18}F]F^- was eluted and dried as with the production of [^{18}F] SPA-RQ-d_2. The oil bath was lowered and after ~30 seconds a solution of 5 μL of bromoethyl triflate [69] in 0.7 mL of o-dichlorobenzene was added, the oil bath was raised and an argon flow was used to

distill the [^{18}F]FCH$_2$CH$_2$Br that forms into a vial at 0°C that contains 0.3 mg of (2S,3S)-1-t-butoxycarbonyl-2-phenyl-3-[2-hydroxy-5-(5'-trifluoro-methyltetrazo-1-yl)phenylmethylene-amino]-piperidine) in 0.2 mL of DMF and ~ 1-2 mg of cesium carbonate. After the amount of radioactivity in the reaction vial peaked, the distillation was stopped and the reaction vial was heated at 110°C for 10 minutes. The removal of the DMF, the deprotection using TFA and the dilution/prep HPLC purification was carried out as with [^{18}F]SPA-RQ-d$_2$. Specific activities of the tracers were 440-4740 Ci/mmol with >98% purity (n = 4).

AT$_1$ ([^{11}C]L-159,884 and [^{18}F]FMe-L-159,884-d$_2$). Preparation of [^{11}C]L-159,884 was performed according to the procedures described by Hamill et al. [50]. Specific activities of the tracers were 341 – 617 Ci/mmol with >98% radiochemical purity (n = 3).

Synthesis of [^{18}F]FMe-L-159,884-d$_2$ was conducted using [^{18}F]FCD$_2$Br as described in the synthesis of [^{18}F]SPA-RQ-d$_2$. The reaction was carried out at 100°C for five minutes. The reaction was diluted with H$_2$O (0.8mL) and purified by preparative HPLC (Phenomenex C18 5μ, 10 x 150 mm, 5 mL/minute,20 minute linear gradient 20:70 to 60:40 acetonitrile: 0.01M NaH$_2$PO4). The desired product elutes at ~ 11.3 minutes. Specific activities of the tracers were estimated from the peak areas of L-159,884 as no standard was available for FMe-L-159,884-d$_2$. Specific activity was ~ 7500 Ci/mmol for the tracers (n = 4) with >98% radiochemical purity.

4.2 Reagents and Materials

Acetonitrile (HPLC grade) was obtained from Fisher Scientific (Fair Lawn, NJ, USA) or Sigma-Aldrich (St. Louis, MO, USA). Formic acid (99%), NADPH, glucose-6-

phosphate, and glucose-6-phosphate dehydrogenase were obtained from Sigma-Aldrich (St. Louis, MO, USA). Heparinized control human and rhesus monkey plasma were obtained from Biological Specialty Corporation (Lansdale, PA, USA). Heparinized control beagle dog plasma was purchased from Innovative Research (Southfield, MI, USA). Human, beagle dog, and rhesus monkey liver microsomes and 0.5M phosphate buffer (pH 7.4) were obtained from BD Biosciences (Woburn, MA, USA).

4.3 Equipment

The HPLC system consisted of two Shimadzu LC-10AD VP pumps and a Shimadzu SIL-HTC autosampler (Columbia, MD, USA). The radiochemical detector was an IN/US Systems 3A Posi (Tampa, FL, USA). The mass spectrometer used for confirmation of the identity of tracers and metabolites was a PE Sciex API 4000 (Thornhill, Ontario, Canada) equipped with a turbo ionspray source. Radiochemical data were processed using Laura Lite 3 (IN/US) software on a Windows 98 platform and mass spectrometer data were processed using PE Sciex Analyst software (version 1.4). For plasma protein binding determinations, Ultrafree-MC Low Binding Cellulose (5000 NMWL) centrifugal filter tubes were purchased from Millipore (Billerica, MA, USA). Ultrafree MC Biomax 5 centrifuge filters (5000 NMWL) were from Millipore and were used to prepare protein-free plasma. Radioactive samples were counted on a Wallac 1470 Wizard Automatic Gamma Counter from Perkin Elmer Life and Analytical Sciences (Wellesley, MA, USA).

4.4 Instrumental Conditions

mGluR5 ([^{18}F]F-PEB). Two HPLC methods were used for the analysis of rhesus monkey plasma samples and in vitro metabolism samples. In both cases, the mobile phase consisted of 0.1% formic acid (A) and acetonitrile (B). For Method A, the analytical separation of [^{18}F]F-PEB from metabolites was performed on a Phenomenex Luna C18 column (4.6 × 50 mm, 3.5 μm). The analytes were separated using a linear gradient with a starting mobile phase composition of 80% A changing linearly to 5% A over 5 minutes and holding at 5% A for 3 minutes. The column was re-equilibrated in the initial conditions for 3 minutes prior to the next sample. The flow rate was 0.5 mL/min and the column was heated to 40°C. For Method B, the analytical separation was performed using a Phenomenex Onyx Monolithic C18 (4.6 × 50 mm) column. A linear gradient consisted of a starting mobile phase composition of 100% A, a 0.1 min linear gradient to 80% A, followed by a 2 min linear gradient to 5% A. The column was re-equilibrated in the initial conditions for 0.5 min. The flow rate was 2 mL/min and the column temperature was held at 40°C. For Method B, the total run time was 3 minutes. Analyte confirmation was performed with detection by tandem mass spectrometry using a turbo ionspray source in positive ion mode. Precursor → product ion transitions for F-PEB (m/z 223.2 → m/z 169.0) were monitored in multiple reaction monitoring (MRM) mode. For Method B, the autosampler wash solvent was also optimized to prevent precipitation of plasma proteins on the autosampler needle and injection port. The wash solvent was used for all studies and consisted of 95/5 formic acid (0.1%)/acetonitrile (v/v).

AT_1 ([^{11}C]L-159,884, [^{18}F]FMe-L-159,884-d_2). The HPLC conditions used for the analysis of in vitro metabolism samples were the same for both tracers. The HPLC solvents consisted of 0.1% formic acid (A) and acetonitrile (B). The column was a Phenomenex Onyx Monolithic C18 (4.6 × 50 mm). The tracers were separated from their metabolites using a linear gradient at 2 mL/min and 40 °C. The starting mobile phase composition was 95% A, changing linearly to 10% A in 2 min, and holding at 10% A for 0.1 min. The column was re-equilibrated in the initial conditions for 0.5 min. The total run time was 2.5 min. Analyte confirmation was performed using tandem mass spectrometry with a turbo ionspray source in positive ion mode. Precursor → product ion transitions for L-159,884 (m/z 555.3 → m/z 134.8) and FMe-L-159,884 (m/z 575.5 → m/z 155.1) were monitored in multiple reaction monitoring (MRM) mode.

NK_1 ([^{18}F]SPA-RQ, [^{18}F]SPA-RQ-d_2, [^{18}F]FESPA-RQ). Analytical conditions were the same for in vitro and in vivo samples. For all three tracers, the HPLC solvents consisted of 0.1% formic acid (A) and acetonitrile (B) and the column was a Waters Xterra MS C18 (50 × 4.6 mm), the flow rate was 0.5 mL/min and the column temperature was 40 °C. For the three tracers, the gradient consisted of a starting composition of 90% A, changing linearly to 20% A over 5 min, and holding at 20% A for 1 min. The column was re-equilibrated in the initial conditions for 3 min. Analyte confirmation was performed using tandem mass spectrometry with a turbo ionspray source in positive ion mode. Precursor → product ion transitions for SPA-RQ (m/z 450.6 → m/z 160.1) and FESPA-RQ (m/z 465.3 → m/z 160.1) were monitored in multiple reaction monitoring (MRM) mode.

[^{18}F]Tracer O. The HPLC conditions were the same for the analysis of in vitro and in vivo metabolism samples. The HPLC solvents consisted of 0.1% formic acid (A) and acetonitrile (B) using a Phenomenex Onyx Monolithic C18 (50 × 4.6 mm) column with a flow rate of 2 mL/min and column temperature of 40 °C. The gradient consisted of a starting mobile phase composition of 95% A for 0.1 min, changing linearly to 30% A over 1.9 min, and holding at 30% A for 0.1 min. The column was re-equilibrated in the initial conditions for 0.4 min. The total run time was 2.5 min. For analysis of in vitro metabolism samples for metabolite identification, the same solvents were used as above. The column was a Waters Xterra MS C18 (50 × 4.6 mm) with a flow rate of 0.5 mL/min and the same column temperature. The gradient consisted of a starting composition of 90% A, changing linearly to 30% A over 5 min, and holding at 30% A for 1 min. The column was re-equilibrated in initial conditions for 3 min. Analyte confirmation was performed using tandem mass spectrometry with a turbo ionspray source in positive ion mode. Precursor → product ion transitions for Tracer O (m/z 415.9 → m/z 193.1) were monitored in multiple reaction monitoring (MRM) mode. For identification of metabolites, the mass spectrometer was operated in Q1 mode, scanning from m/z 100 to m/z 500 during the course of the HPLC run. This allowed for identification of molecular ions from HPLC peaks for the metabolites.

[^{18}F]TracerMG. The following HPLC conditions were used for the analysis of in vivo metabolism samples from rhesus monkey plasma. The HPLC solvents were 0.1% formic acid (A) and acetonitrile (B) using a Waters Xterra MS C18 column (50 × 4.6 mm) with a flow rate of 0.5 mL/min and temperature of 40°C. The gradient consisted of a starting composition of 80% A, changing linearly to 10% A over 5 min, and holding at

10% A for 1 min. The column was re-equilibrated in the initial conditions for 3 min. Analyte confirmation was performed by tandem mass spectrometry using a turbo ionspray source in positive ion mode. Precursor → product ion transitions for Tracer MG (m/z 352.4 → m/z 227.3) were monitored in multiple reaction monitoring (MRM) mode.

4.5 Rhesus Monkey In Vivo Metabolism - Plasma Sample Analysis

All studies in rhesus monkeys were conducted under the guiding principles of the American Physiological Society and the *Guide for Care and Use for Laboratory Animals* published by the US National Institutes of Health (NIH publication No 85-23, revised 1985). All studies were approved by the West Point Institutional Animal Care and Use Committee at Merck Research Laboratories. In all cases, rhesus monkeys were initially anesthetized with ketamine (10 mg/kg, i.m.), then induced with propofol (5 mg/kg i.v.), intubated and respired with medical grade air. Venous blood samples were collected 3, 5, 15, 30, 45, 60 and 90 min after the injection of ~ 2-5 mCi of the appropriate tracer. No in vivo metabolism studies were conducted for the AT_1 PET tracers.

mGluR5 ([^{18}F]F-PEB). Plasma samples were collected from six different rhesus monkeys. In some cases, a baseline PET scan was performed after the injection of [^{18}F]F-PEB for 90 min, followed by administration of a blocking drug and another dose of [^{18}F]F-PEB. In this case plasma samples were collected after both injections of [^{18}F]F-PEB. In all cases, approximately 0.5 – 1 mL of blood was collected from the monkey. The blood was immediately centrifuged at 5433 ×*g* for 90 seconds and the plasma (0.2 – 0.4 mL) was aliquotted to a 1.5 mL microcentrifuge tube. For samples analyzed using Method A, the plasma was immediately treated with 0.4 mL acetonitrile, briefly vortexed,

and centrifuged at 5433 ×*g* for 90 seconds. The acetonitrile was transferred to an autosampler vial. For later time points, the acetonitrile was evaporated to approximately 0.1 – 0.2 mL to concentrate the samples. For samples analyzed using Method B, the plasma was diluted with an equal volume of 0.1% trifluoroacetic acid, briefly vortexed, and centrifuged at 5433 ×*g* for 90 seconds, then transferred to an autosampler vial. A 100 μL aliquot was injected for analysis by either method with detection by the radiochemical detector.

NK_1 ([^{18}F]SPA-RQ, [^{18}F]SPA-RQ-d_2, [^{18}F]FESPA-RQ). Blood samples were collected from five different monkeys, with multiple studies performed in Monkey C. Only one in vivo study was performed with [^{18}F]FESPA-RQ. Three studies each were performed with either [^{18}F]SPA-RQ or [^{18}F]SPA-RQ-d_2. In all cases, blood samples (~0.5 - 1 mL) were collected after a ~5 mCi bolus injection of tracer at the time points described above. The blood was immediately centrifuged at 5433 ×*g* for 90 seconds and the plasma (0.2 – 0.4 mL) was aliquotted to a 1.5 mL microcentrifuge tube. The plasma was treated with 0.4 mL acetonitrile and centrifuged at 5433 ×*g* for 90 seconds. The acetonitrile was transferred to an autosampler vial and 100 μL was injected onto the HPLC system for analysis with detection by the radiochemical detector.

[^{18}F]Tracer O. The studies consisted of a ~ 5 mCi bolus injection of [^{18}F]Tracer O in two different monkeys, with duplicate studies in each monkey. Venous blood samples were collected at the time points described above. The whole blood (~0.5 – 1 mL) was centrifuged for 90 sec at 5433 ×*g*. The plasma (~0.2 – 0.5 mL) was removed and combined with 200 μL of 0.1% TFA. The samples were briefly vortexed then centrifuged at 5433 ×*g* for 90 sec and the mixture was transferred to an HPLC autosampler vial. An

aliquot (100 μL) of the sample was injected onto the HPLC system for analysis with detection by the radiochemical detector.

After in vitro metabolism of [^{18}F]Tracer O to produce the [^{18}F]-labeled metabolites, ~2 – 5 mCi of the [^{18}F]-labeled metabolites were injected in one monkey. Venous blood samples were collected 3, 5, 15, 30, 45, and 60 min after the injection of tracer. Two studies were performed in one monkey. In one study, plasma samples were only collected up to 30 min and the PET scan stopped at 35 min due to issues with anesthesia. Plasma was collected and treated as described for [^{18}F]Tracer O. Images from the PET studies were evaluated for uptake of the labeled metabolites in the brain, and compared to data previously obtained for the parent tracer.

[^{18}F]Tracer MG. Several studies were performed in two different rhesus monkeys. The first set of studies (n = 2 in two monkeys) included a baseline scan after a ~5 mCi bolus injection of [^{18}F]Tracer MG. The second set of studies were performed in the same two monkeys and included a bolus followed by infusion of blocking drug (BD) for 1 hour prior to a ~5 mCi bolus injection of the tracer. For Monkey A, the blocking drug was a 1.8 mpk bolus injection followed by a 0.72 mpk/hr infusion for 1 hour. For Monkey B, the blocking drug was a 0.9 mpk bolus injection followed by 0.36 mpk/hr infusion for 1 hour. In all cases, venous blood samples were collected at the time points described above. The whole blood was centrifuged for 90 sec at 5433 ×*g*. The plasma (~ 200 μL) was removed and protein precipitated by the addition of 400 μL of acetonitrile. The samples were briefly vortexed then centrifuged at 5433 ×*g* for 90 sec and the acetonitrile was transferred to an HPLC autosampler vial. An aliquot of the sample (100 μL) was injected onto the HPLC system for analysis with detection by the radiochemical detector.

4.6 In Vitro Metabolism Studies

In vitro metabolism studies were performed in rhesus monkey, human, or beagle dog liver microsomes purchased from BD Biosciences (Franklin, MA, USA). Each of the tracers was diluted in 1 mL phosphate buffer (0.1 M, pH 7.4) to counts ranging from 0.371 – 2 mCi/mL). The incubation mixture (1 mL) contained 0.2 mg/mL monkey, human, or beagle dog liver microsomes, 10 μL of a 10× NADPH regenerating solution, 0.1M phosphate buffer (pH 7.4), 6 mM $MgCl_2$, and 10 μL of solution containing the tracer. The 10× NADPH regenerating solution contained 1 mM NADP, 25 U/mL glucose-6-phosphate-deghydrogenase, 100 mM glucose-6 phosphate prepared in 0.1 M phosphate buffer (pH 7.4). The reaction was started by the addition of NADPH and samples were incubated at 37°C for one hour. Aliquots of the mixture (0.2 mL) were removed 5, 15, 30 and 60 min during the incubation. In some cases, the 15 min sample was omitted. Each aliquot was combined with 0.2 mL acetonitrile to stop the reaction and analyzed using the methods described above. Metabolism was evaluated by measurement of radioactive peaks. Metabolism in beagle dog liver microsomes was only evaluated for the AT_1 PET tracers.

[^{18}F]Tracer O.

Evaluation of Metabolite Structure and Comparison of Rates of Metabolism

The procedures described above were used to determine the structure of the labeled metabolites. The incubation mixture contained 1 μM of unlabeled Tracer O in addition to [^{18}F]Tracer O. The methods were also used to determine whether the metabolites present in monkey would also be likely to be present in human subjects.

Preparation of Labeled Metabolites for In Vivo Monkey Study

In vitro metabolism was used to prepare [^{18}F]-labeled metabolites of [^{18}F]Tracer O for an in vivo monkey imaging study. Several conditions were evaluated for optimal production of the labeled metabolites. Ultimately, five sets of incubations were prepared in parallel. Each incubation was prepared in a 5 mL polypropylene test tube and contained approximately 8 mCi of [^{18}F]Tracer O, 1.3 mM NADP+, 3.3 mM glucose-6-phosphate, 3.3 mM MgCl2, 0.4 U/mL glucose-6-phosphate dehydrogenase, 2 mg/mL of rhesus monkey liver microsomes, and 0.1 M phosphate buffer (pH 7.4) in a total volume of 1 mL. Each tube was incubated in a shaking water bath at 37°C for 30 min. At the end of the incubation, the mixtures were pooled in the barrel of a 5 mL syringe with a C18 Sep-Pak Light cartridge attached (Waters, Milford, MA, USA). The cartridges were first conditioned with acetonitrile followed by DI water. After the incubation mixture was passed through the cartridge, the cartridge was washed with 5 mL of DI water. The labeled metabolites were eluted with 150 μL of ethanol 2-3 times. The ethanol was diluted with DI water to a final volume of 1.2 mL. The mixture was injected onto an HPLC system and separated on a Phenomenex C18 Gemini column (10 × 150 mm, 5 μm). The mobile phase consisted of 0.1% TFA (A) and acetonitrile (B) and the metabolites were eluted using a 20 min linear gradient from 80% A to 10% A. Fractions were collected from 4 – 4.5 min into a sterile vial.

4.7 Plasma Protein Binding

Protein binding was evaluated in rhesus monkey and human plasma for all tracers except [^{18}F]Tracer O, as well as beagle dog plasma for the AT_1 tracers. In all cases,

control plasma was purchased elsewhere. For [^{18}F]Tracer MG, plasma was obtained from the monkeys during the bolus+infusion protocol of the PET studies. The centrifugal filters were pre-treated with 0.1 mL of 10 μM of cold tracer to prevent non-specific binding of the tracers to the filters. The tubes were centrifuged at 5000 × g for 30 min at 37°C. The cold tracer was removed from the collection tube as well as any residual solution that did not pass through the filters. Protein-free plasma was prepared in order to correct for binding of the tracers to the centrifugal filters. Protein-free plasma was prepared by centrifugation of control plasma in filters with a 5000 molecular weight cutoff. In all cases, 0.2 mL of control plasma (heparinized or protein-free) was treated with 0.01 mL of 0.16 – 1.2 mCi of the appropriate tracer and incubated for 30 min at 37°C. After the incubation, a 20 μL aliquot of plasma was transferred to a scintillation vial and counted by gamma counter for determination of counts in total plasma. The remaining plasma was transferred to the low-binding cellulose centrifugal filters and centrifuged at 5000 × *g* for 30 min at 37°C. A portion of the free fraction (0.02 mL) was transferred to a scintillation vial and counted. All counts were decay-corrected to the start time of the incubation. Protein binding was calculated from the fraction of counts in the total plasma and free fraction. All calculations of protein binding were corrected for non-specific binding of the tracer to the centrifugal filters using the following equations:

Equation 5: $$\text{Fraction Unbound } (f_u) = \frac{\text{Counts in Free Fraction}}{\text{Counts in Total Plasma}}$$

Equation 6: $$\text{Plasma Free Fraction } (\%) = (1 - (f_u \text{ Sample} * f_u \text{ Control})) * 100$$

For [^{18}F]Tracer MG, plasma was obtained from a rhesus monkey prior to the bolus injection of the blocking drug and at the end of the 60 min infusion. The tracer (10 μL of

~800 μCi) was added to the plasma and incubated at 37 °C for 30 min. All other procedures were as described above.

5. Results and Discussion

5.1 mGluR5 ([^{18}F]F-PEB)

5.1.1. In Vivo Metabolism – Rhesus Monkey Plasma

Plasma samples were collected during PET studies and analyzed for metabolism of [^{18}F]F-PEB from six different monkeys, with duplicate studies in several monkeys. Representative chromatograms for plasma samples analyzed by both Method A and Method B are shown in Figure 8. The chromatograms are from samples obtained 60 min after injection of the tracer. Due to the low level of counts in plasma, there is a significant level of noise in the baseline of the chromatogram but peaks were still able to be integrated. There were no significant differences in the results obtained using either Method A or Method B and in each case, four labeled metabolites were observed. The main advantage to using Method B is the fast analysis time (2.5 min) and minimal sample pre-treatment due to the use of the monolithic column. Thus, sample analysis time was reduced both in sample preparation and HPLC analysis. Plasma was diluted with trifluoroacetic acid (0.1%) and injected directly onto the HPLC system. Due to the presence of plasma proteins, the injector wash was optimized to prevent precipitation either in the injection needle or in the injection port. A predominantly aqueous wash consisting of 95/5 formic acid (0.1%)/acetonitrile (v/v) was used to prevent precipitation of any plasma protein and to clean and rinse the injector needle and port. The fast

analysis time used with this method allows for the possibility of rapid blood sampling if required in future studies, such is the case when a more accurate determination of the shape of the curve for activity and metabolism of a tracer in plasma is required in tracer modeling. Fast analysis times are also an advantage when a tracer is labeled with ^{11}C due its short half-life.

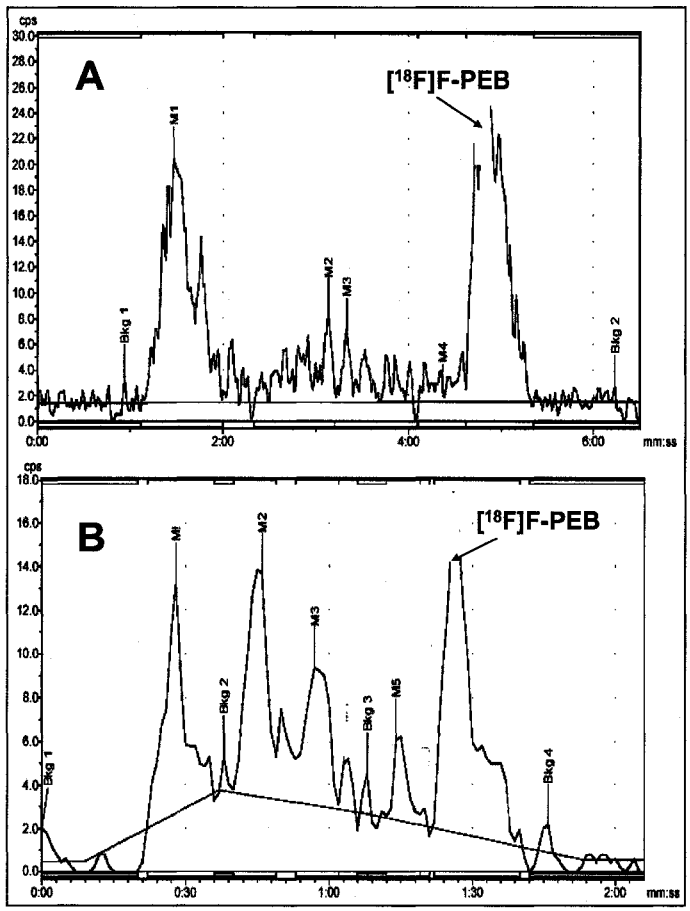

Figure 8. Representative radiochromatograms used to evaluate the metabolism of [^{18}F]F-PEB in rhesus monkey plasma. Both chromatograms were from samples obtained 60 min after injection of tracer.

A: Samples analyzed using Method A

B: Samples analyzed using Method B

Metabolism was evaluated by the percent total radioactivity due to parent tracer over time as shown in Figure 9. After 90 min, approximately 40-80% of the total radioactivity was due to [^{18}F]F-PEB. All of the metabolites were more polar than the parent tracer and would not be likely to enter the brain. Some variability exists in the measurements of metabolism in the monkey studies. This variability is common to in vivo studies and could be due to a number of factors such as differences in specific activity of the tracers, anesthesia that the monkeys received during the studies, or age, size, and gender of the monkeys. Overall, in vivo metabolism is not a limiting factor in the use of this PET tracer for imaging the mGluR5 receptors, at least in the monkey brain. At the end of a normal PET scan (generally 90 min), sufficient parent tracer is circulating in the blood and based on their relative polarity to the parent tracer, none of the metabolites are likely to cross the blood-brain barrier.

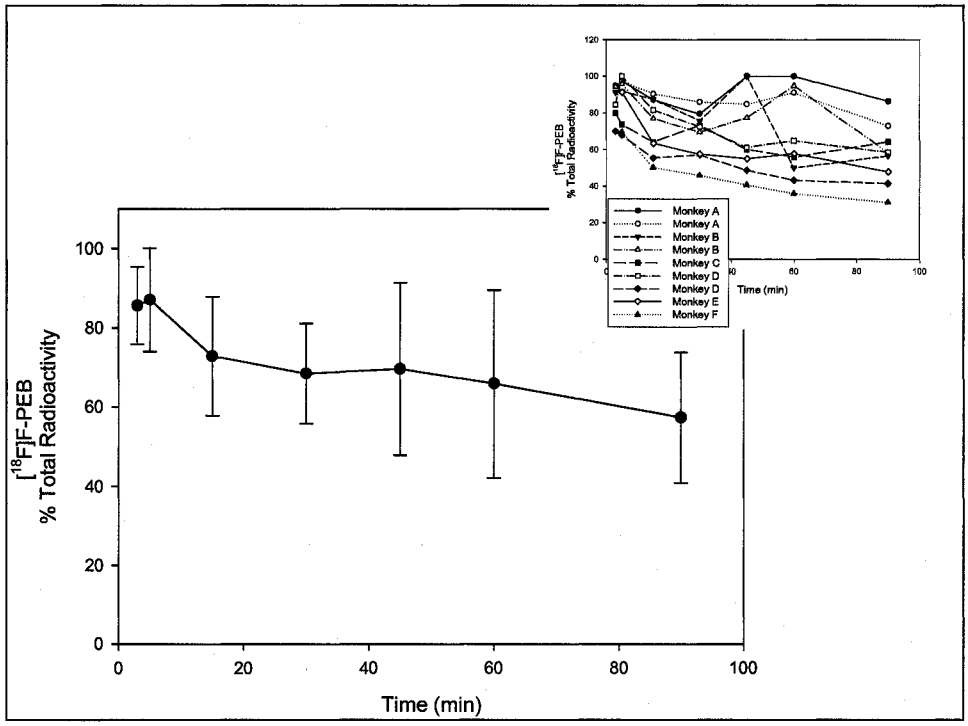

Figure 9. Metabolism of [^{18}F]F-PEB in rhesus monkey plasma plotted as mean percent total radioactivity at each time point (n = 9). Error bars are standard deviation of the measurement for all the monkeys at each time point. Inset figure shows individual plots of metabolism for each monkey studied.

5.1.2. In Vitro Metabolism Studies

In vitro metabolism was evaluated in several lots of rhesus monkey (MLM) and human (HLM) liver microsomes. The results are summarized in Figure 10. A slightly overall faster rate of metabolism was observed in human than in rhesus monkey liver microsomes. After 60 min >20% of the total radioactivity was due to [^{18}F]F-PEB in HLM and >50% in MLM. Based on mass spectrometric analysis, the observed metabolites were similar in microsomes from both species as well as to the in vivo plasma samples as measured by retention times on the chromatograms and were most likely due to hydroxylation of the parent tracer. The greater variability in the metabolism in HLM is thought to be due to the use of different lots of pooled human liver microsomes. Although

the microsomes were purchased commercially, slight differences always exist in enzyme activity between lots, particularly for human microsomes. These differences could contribute to the variable rate of metabolism between studies.

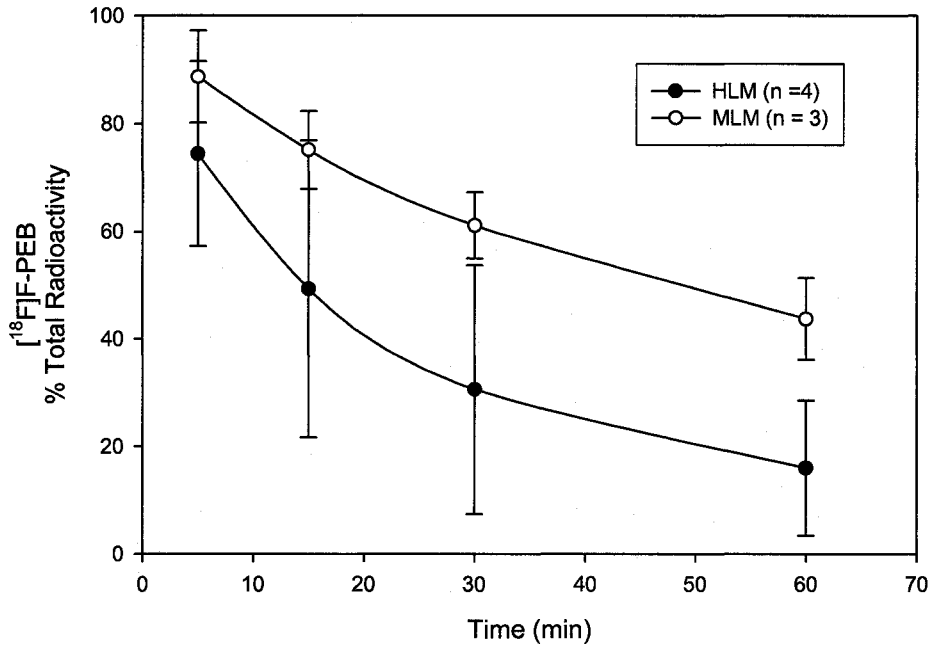

Figure 10. In vitro metabolism of [^{18}F]F-PEB in human (HLM) and rhesus monkey (MLM) liver microsomes reported as mean percent total radioactivity at each time point. Error bars are standard deviations of the measurements at each time point from the different studies (n = 4 for HLM, n = 3 for MLM).

Hamill et al. [35] described the preclinical development of [^{18}F]F-PEB and two other potential tracers for imaging the mGluR5 receptors. One difference from the results reported here and the Hamill paper is in the relative rates of metabolism in vitro. The in vitro metabolism experiments reported in the paper stated that slower metabolism of the unlabeled tracer by human liver microsomes was observed compared with monkey liver microsomes, which is the reverse of what is reported here. In the Hamill paper, all of the

in vitro metabolism experiments were conducted with unlabeled tracer at a concentration of 1 μM [35]. The discrepancy between the results reported in the paper and those reported herein could be due to the use of higher concentration of unlabeled F-PEB in the studies reported by Hamill et al. [35]. All experiments reported here were conducted with labeled tracer and, using the specific activities, the concentration of F-PEB in the incubations was ~0.1 – 0.3 μM. In order to determine whether the increased mass of F-PEB could lead to changes in the relative rates of metabolism in vitro, one experiment was performed in which enough unlabeled F-PEB was added to the incubation along with the labeled tracer to equal 1 μM. A significant difference in the rate of metabolism was observed for both species. At 60 min, 84% of the total radioactivity was due to [^{18}F]F-PEB in MLM and 89% in HLM.

This difference could explain the discrepancy in metabolism between what is reported here based on tracer alone and what was reported by Hamill et al. [35] using the unlabeled tracer at a higher concentration. These results highlight the importance of conducting these types of experiments at tracer level as opposed to levels more traditionally used in drug metabolism studies, especially considering in vivo studies are conducted at low mass.

5.1.3. Plasma Protein Binding

Protein binding of [^{18}F]F-PEB was evaluated in several different lots of human and rhesus monkey plasma. The results are summarized in Figure 11. There is no significant difference in the protein binding of this tracer in human or rhesus monkey plasma. The free fraction was 8.2% ± 0.5% for monkey and 8.1% ± 0.7% for human. Nonspecific

binding of the tracer to the centrifugal filter was 35.2% for monkey and 36.4% for human. The coefficient of variation (CV%) for the measurement of free fraction, or nonspecific binding, in the protein-free plasma was ≤4.8% for both species. Thus, all measurements were corrected for nonspecific binding of the tracer.

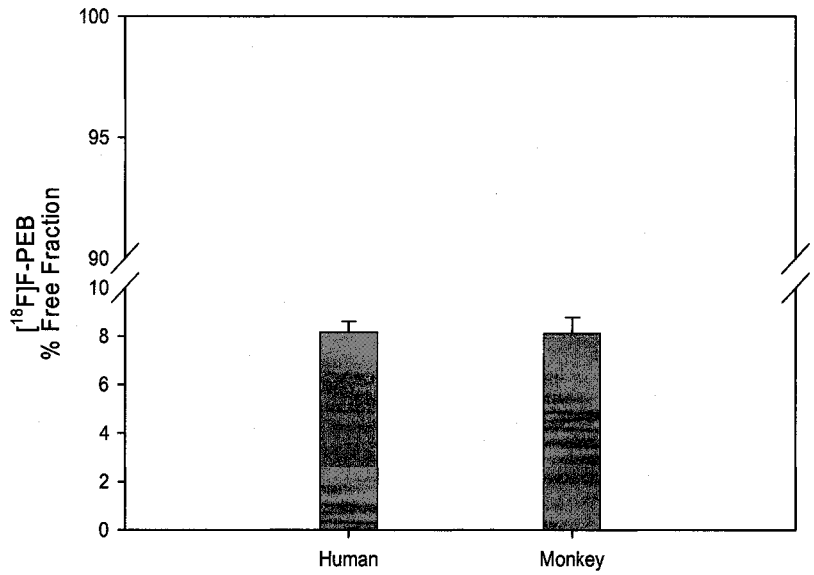

Figure 11. Protein binding of [^{18}F]F-PEB in rhesus monkey and human plasma. Results are reported as percent tracer found in the free fraction. Error bars are the standard deviation for the individual measurements (n = 4).

Results from PET studies in rhesus monkeys indicated that [^{18}F]F-PEB exhibited a long-lived specific signal in the brain. The tracer also reached equilibrium within the time of a typical PET study [35]. Furthermore, the mGluR5 specificity of [^{18}F]F-PEB was confirmed by both in vivo and in vitro experiments [35]. Based on the results from PET studies, further development of [^{18}F]F-PEB, particularly in human studies was warranted. Based on the in vitro metabolism results using [^{18}F]F-PEB, one might expect slightly faster metabolism of the tracer in vivo in human studies. However, even during a 90 min

scan, the parent tracer would be expected to be intact in human subjects given the results of in vivo metabolism in monkeys. Furthermore, none of the labeled metabolites would be likely to cross the blood-brain barrier, nor confound the PET signal. Plasma protein binding is not likely to be a deterrent to the use of this tracer in human subjects, as it behaves similarly in both monkey and human. Development activities to support human clinical studies using [^{18}F]F-PEB to image mGluR5 receptors in vivo are currently ongoing.

5.2 AT$_1$ ([^{11}C]L-159,884 and [^{18}F]FMe-L-159,884-d$_2$)

5.2.1. In Vitro Metabolism

In vitro metabolism was evaluated for both [^{11}C]L-159,884 and [^{18}F]FMe-L-159,884-d_2 in human, beagle dog, and rhesus monkey liver microsomes. Metabolism was determined from the peak areas of the radioactive peaks and was reported as percent total radioactivity at a given time (Figure 12). For [^{11}C]L-159,884, there was no significant difference in the in vitro metabolism of the tracer between the species with approximately 30-40% of the radioactivity due to parent tracer after incubation for 60 min. However, for [^{18}F]FMe-L-159,884-d_2, metabolism was significantly slower in dog and human liver microsomes than in monkey liver microsomes. After incubation for 60 min, approximately 60-70% of the radioactivity was due to [^{18}F]FMe-L-159,884-d_2 in human and dog with only approximately 20% in monkey. There was no significant difference in the rate of metabolism between the dog and human for both tracers. Comparing the two tracers, relative rates of metabolism were dog $\approx$ human $\approx$ monkey for [^{11}C]L-159,884 and

dog ≈ human < monkey for [^{18}F]FMe-L-159,884-d_2. Based on these findings, one would predict [^{18}F]FMe-L-159,884-d_2 may be more metabolically stable in vivo in human studies than [^{11}C]L-159,884.

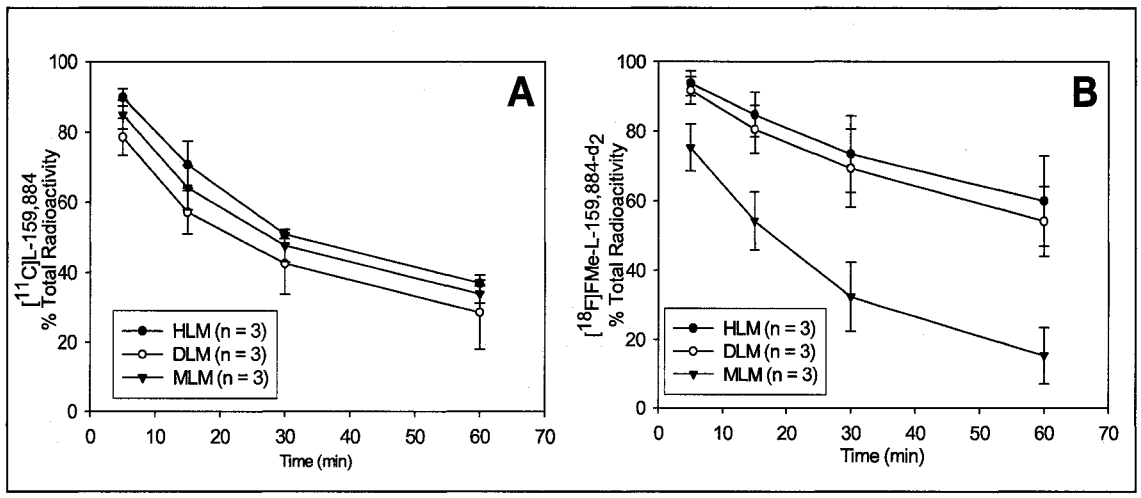

Figure 12. In vitro metabolism of [^{11}C]L-159,884 (A) and [^{18}F]FMe-L-159,884-d_2 (B) in human (HLM), beagle dog (DLM), and rhesus monkey (MLM) liver microsomes. Error bars are standard deviations for the measurements at each time point.

In vitro metabolism of both tracers resulted in four labeled metabolites, all more polar than the parent compound. Representative chromatograms for each tracer are shown in Figure 13. Based upon mass spectrometric analysis of the metabolites, the main labeled metabolites are similar for both tracers and their structures are dealkylation products of the parent tracer.

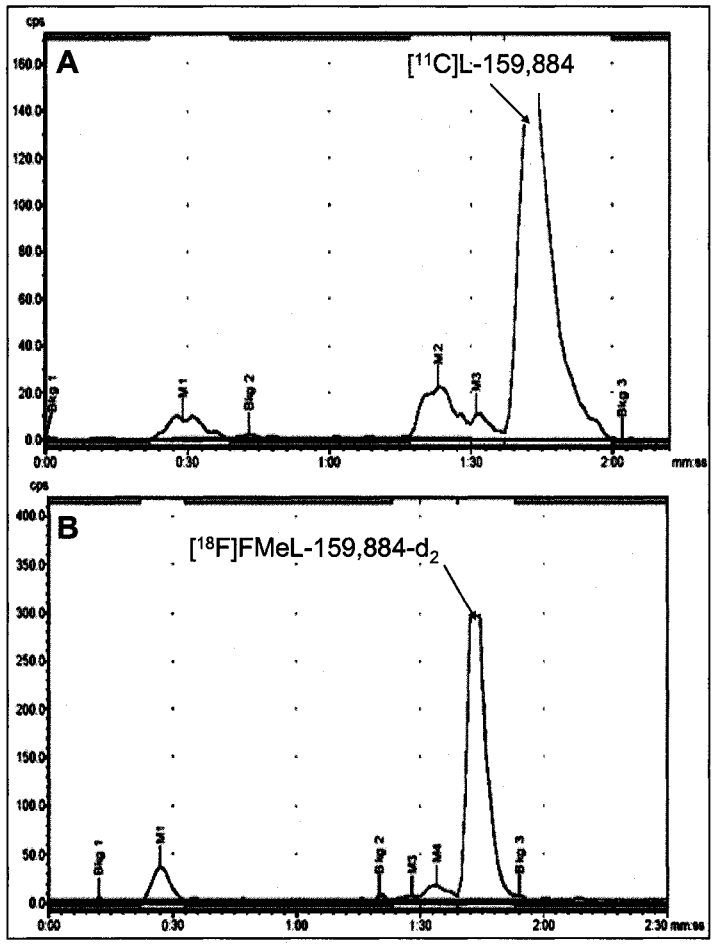

Figure 13. Representative radiochromatograms for the in vitro metabolism of [^{11}C]L-159,884 **(A)** and [^{18}F]FMe-L-159,884-d_2 **(B)** in human liver microsomes after 30 min incubation at 37°C.

5.2.2. Plasma Protein Binding

Protein binding was evaluated in human, beagle dog, and rhesus monkey plasma. The results are summarized in Figure 14. There was no significant difference between the two tracers in any of the species evaluated. However, there was approximately 3 times more tracer in the free fraction of dog plasma (1.2% ± 0.03%) than in human plasma (0.4% ± 0.03%) for both tracers. The free fraction in monkey plasma was 0.8 ± 0.08% for both tracers. Thus, plasma protein binding was high for both tracers in all species evaluated.

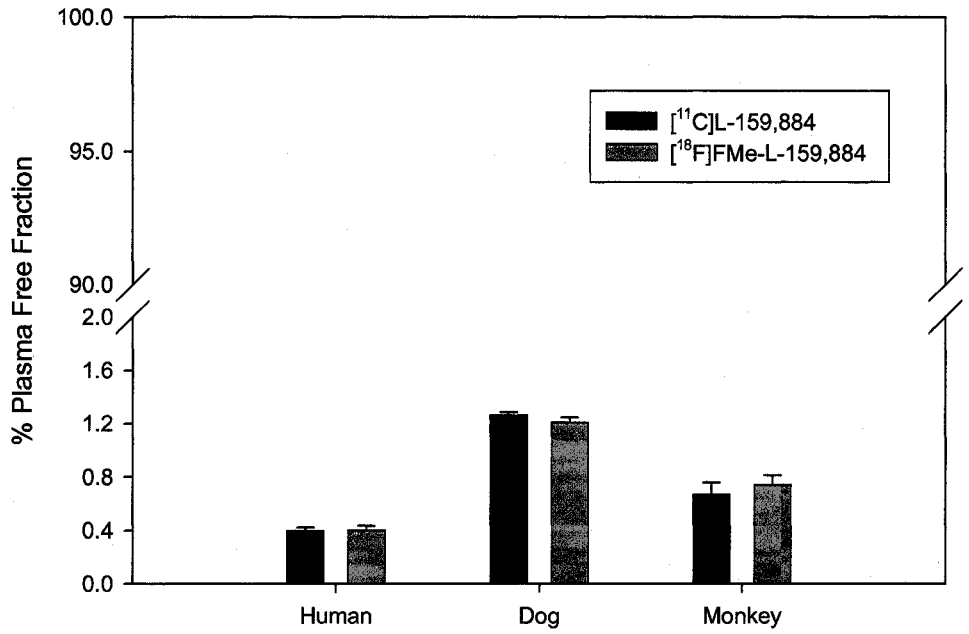

Figure 14. Plasma free fraction (percent) of [^{11}C]L-159,884 and [^{18}F]FMe-L-159,884-d_2 corrected for nonspecific binding to the filters in human beagle dog, and rhesus monkey plasma. Error bars represent the standard deviation of the measurements in each species (n = 4).

Unlabeled tracer (10 μM) was used to pre-treat the filters to prevent non-specific binding of the tracers to the filters in the centrifuge tubes. The use of the unlabeled tracer did not prevent all nonspecific binding as 16.6%, 36.6% and 15.4% of the tracer was bound to the filters for human, dog, and monkey plasma, respectively for [^{11}C]L-159,884. For [^{18}F]FMe-L-159,884-d_2, nonspecific binding to the filters was also apparent with 24.2%, 26.4%, and 19.6% for human, dog and monkey, respectively. Pre-treating the filters with unlabeled tracer did significantly reduce the amount of binding of the labeled tracers to the filters. With no pre-treatment, binding to the filters was >80% for both tracers. The high binding of the labeled tracers to the filters is likely due to the low mass

of compound present in the tracer solution. All measurements using protein-free plasma were reproducible with coefficients of variation (CV%) ≤9.5%. The calculations for free fraction and protein binding were corrected for non-specific binding of the tracer to the centrifugal filter.

[^{11}C]L-159,884 has been used to successfully image the type 1 angiotensin receptors (AT_1) in vivo in dogs and baboons using PET [52, 53, 55]. However, rapid metabolism of [^{11}C]L-159,884 was observed in initial human studies (unpublished results). Plasma protein binding was also evaluated in human, dog, and baboon using dextran-coated charcoal to trap bound ligand [55]. High plasma protein binding was reported for all three species, with human exhibiting the highest binding. The experiments reported here were used to determine whether in vitro techniques such as in vitro metabolism and plasma protein binding would have predicted the failure of the tracer in human studies and whether [^{18}F]FMe-L-159,884-d_2 may have been more successful in human PET imaging studies. The likelihood of success with [^{18}F]FMe-L-159,884-d_2 depends on whether the main reason for failure of [^{11}C]L-159,884 in humans was due to metabolism, plasma protein binding, a combination of both, or some other interaction that is yet to be determined, such as a transport mechanism.

Based on the results reported here, plasma protein binding is relatively equal for both tracers. A 3-fold increase in the free fraction of both tracers was clearly shown between dog and human plasma with dog having the higher free fraction. Thus, if protein binding was the reason for the poor imaging results in humans, then [^{18}F]FMe-L-159,884-d_2 is also not likely to be successful in human imaging studies. However, the in vitro metabolism results show that there is a significant difference in the relative rates of

metabolism between the two tracers in dog and human liver microsomes. If the relative metabolism behaves similarly in vivo in human studies, then [^{18}F]FMe-L-159,884-d_2 may exhibit better stability in vivo.

5.3 NK$_1$ ([^{18}F]SPA-RQ, [^{18}F]SPA-RQ-d_2, [^{18}F]FESPA-RQ)

5.3.1. In Vivo Metabolism – Rhesus Monkey Plasma

Plasma samples were collected during PET studies in several different monkeys, with duplicate analyses in some monkeys. The plasma samples were analyzed for metabolism of [^{18}F]SPA-RQ (n = 3), [^{18}F]SPA-RQ-d_2 (n = 3), and [^{18}F]FESPA-RQ (n = 1) using the radiochemical detector. Representative chromatograms for each of the tracers in plasma are shown in Figure 15.

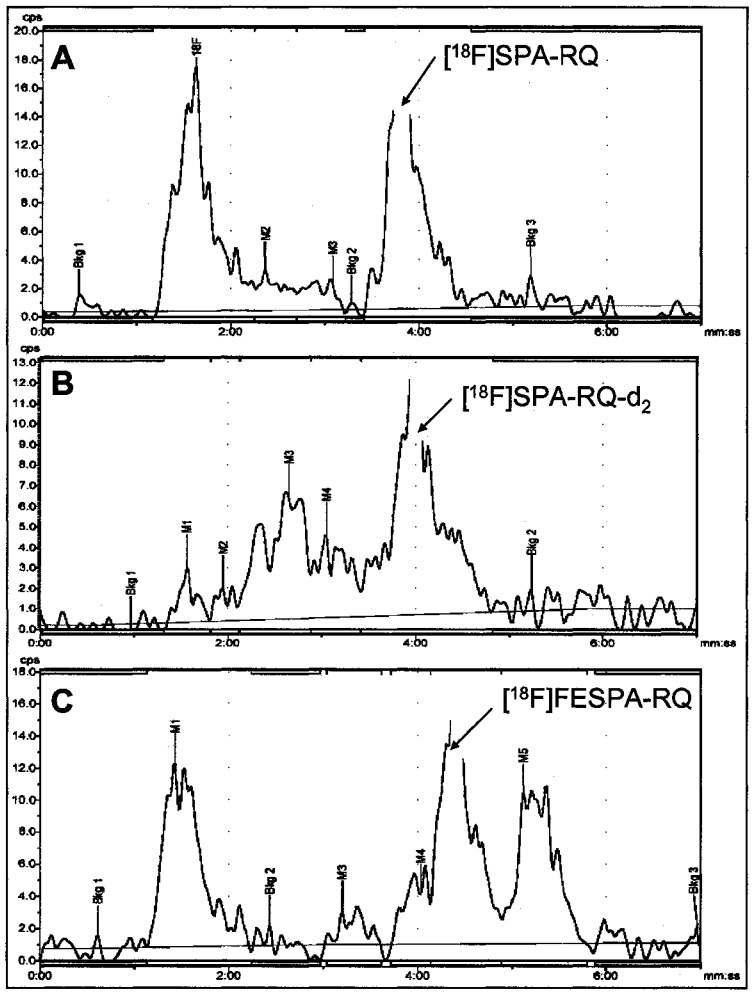

Figure 15. Representative radiochromatograms for the analysis of NK_1 PET tracers in rhesus monkey plasma. All chromatograms are for samples collected 60 min after injection of tracer.

A: [^{18}F]SPA-RQ in Monkey C,

B: [^{18}F]SPA-RQ-d_2 in Monkey C,

C: [^{18}F]FESPA-RQ in Monkey A.

The results were plotted for each tracer as percent total radioactivity over time as shown in Figure 16. For [^{18}F]SPA-RQ, only 3 labeled metabolites were observed, while five labeled metabolites were observed for both [^{18}F]SPA-RQ-d_2, and [^{18}F]FESPA-RQ. In both cases, M5 eluted after the tracer. The more hydrophobic nature of this metabolite

may make it more likely to cross the blood-brain barrier. All other metabolites were more polar than the parent tracer. In most cases, the majority of radioactivity at the end of the PET scan (90 min) was due to defluorination of the tracer as evidenced by the presence of [^{18}F]F- on the HPLC chromatograms (M1 in Figure 15).

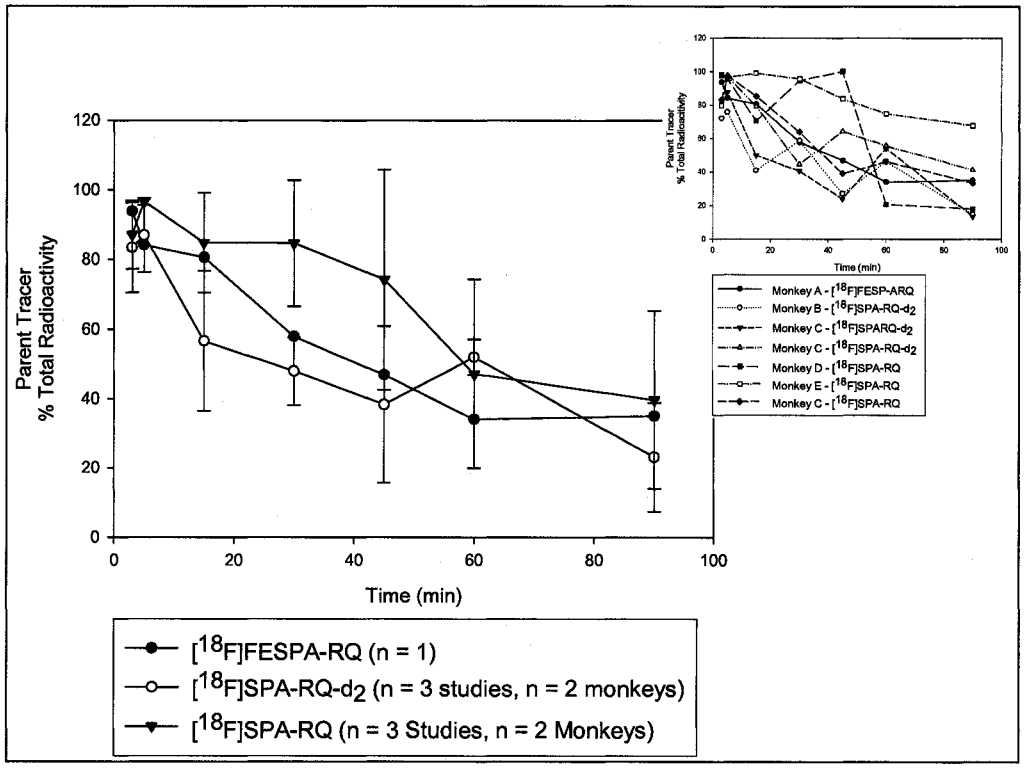

Figure 16. Metabolism of [^{18}F]SPA-RQ, [^{18}F]SPA-RQ-d_2, and [^{18}F]FESPA-RQ in rhesus monkey plasma plotted as mean percent total radioactivity at each time point. Error bars are standard deviation of the measurement for all the monkeys at each time point. Inset figure shows individual plots of metabolism for each monkey and tracer studied.

The presence of [^{18}F]F- for each tracer was plotted as percent total radioactivity over time as shown in Figure 17. The results show the presence of [^{18}F]F- varied for [^{18}F]SPA-RQ-d_2 between the studies and based on the standard deviations, there was no significant difference between the defluorination of [^{18}F]SPA-RQ and [^{18}F]SPA-RQ-d_2.

The defluorination of [^{18}F]FESPA-RQ appears to be slightly less significant, however this was based on only one in vivo monkey study. As described in the Background section, defluorination of [^{18}F]SPA-RQ led to bone uptake of [18F]F- as viewed in the images obtained during early PET studies in monkeys. Thus, the development and evaluation of [^{18}F]SPA-RQ-d_2 and [^{18}F]FESPA-RQ were explored as possible alternatives to [^{18}F]SPA-RQ with the hope that they would be more metabolically stable in vivo and less prone to defluorination. At the time of tracer development, analysis of the metabolism of the labeled tracers was limited to TLC, which provides only a relative measurement of metabolism, and could not distinguish the difference between [^{18}F]F- and other polar labeled metabolites. Based on the results reported here, defluorination appears to be less likely with [^{18}F]FESPA-RQ in vivo which correlates well with the early PET study results discussed in the Background section. In those studies, less bone uptake was observed with [^{18}F]FESPA-RQ than [^{18}F]SPA-RQ. Bone uptake was similar for [^{18}F]FESPA-RQ and [^{18}F]SPA-RQ-d_2.

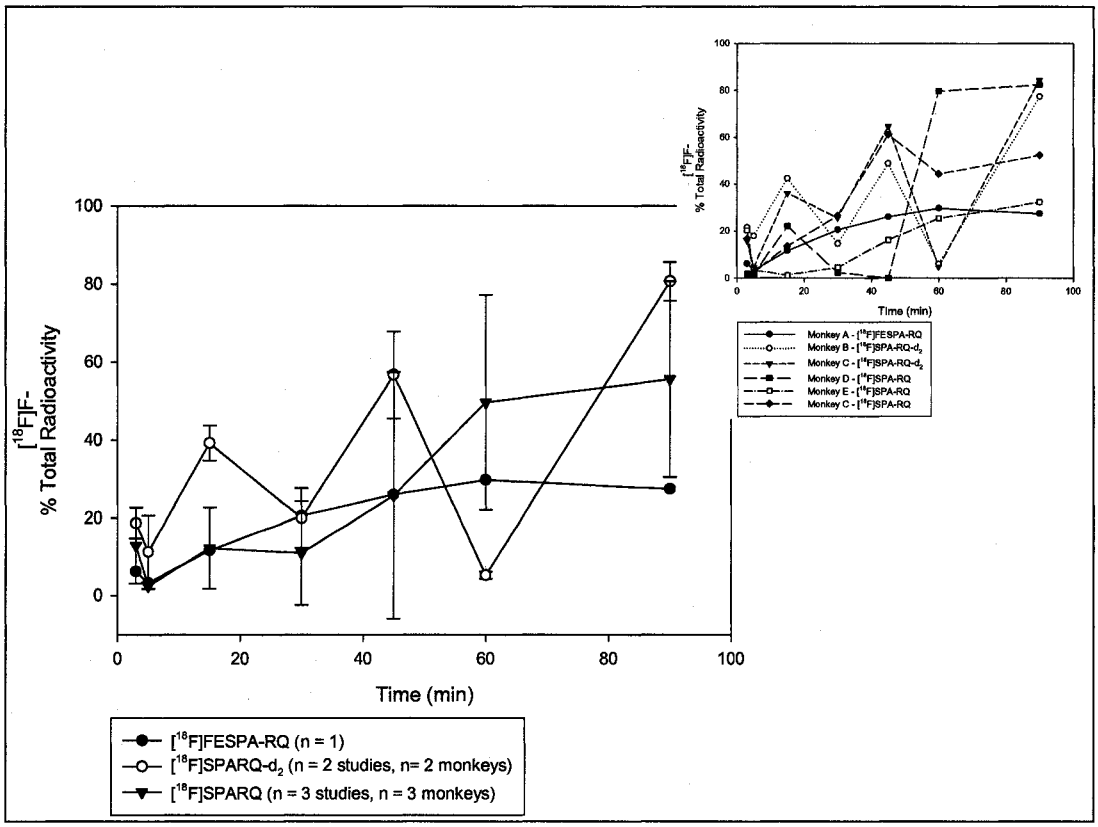

Figure 17. Presence of [^{18}F]F- in rhesus monkey plasma after injection of [^{18}F]SPA-RQ, [^{18}F]SPA-RQ-d_2, and [^{18}F]FESPA-RQ plotted as mean percent total radioactivity at each time point. Error bars are standard deviation of the measurement for all the monkeys at each time point. Inset figure shows individual plots for each monkey and tracer studied.

Metabolism of [^{18}F]SPA-RQ was reported in human subjects by Hietala et al. (2005). Arterial plasma was measured for metabolites with thin layer chromatography and digital autoradiography in one group of patients (n = 4). Eighty minutes after injection of the [^{18}F]SPA-RQ, approximately 30-40% of the radioactivity was due to intact tracer. The presence of an unidentified hydrophilic metabolite was observed by TLC analysis of the plasma samples. The hydrophilic metabolite would be unlikely to cross the blood-brain barrier. Free fluoride was observed by TLC as well. Uptake of radioactivity in the skull was reported for some patients at later scanning times. Brain radioactivity had to be monitored for up to six hours due to slow tracer kinetics. Overall, the in vivo metabolism

results from monkey correspond well with the results reported for the human study. Thus, in this case, monkey in vivo metabolism of [^{18}F]SPA-RQ serves as a good predictor of performance of the tracer in humans.

5.3.2. In Vitro Metabolism

In vitro metabolism of the three NK_1 PET tracers was evaluated in both rhesus monkey and human liver microsomes. The results are summarized in Figure 18. Based on chromatographic retention time, the same metabolites were observed in vitro in both species as was observed in vivo in rhesus monkey plasma. In rhesus monkey liver microsomes, [^{18}F]SPA-RQ-d_2 exhibited the slowest metabolism while [^{18}F]FESPA-RQ experienced the most rapid metabolism. In human liver microsomes, there was very little difference in metabolism between [^{18}F]SPA-RQ and [^{18}F]SPA-RQ-d_2, while both exhibited slower metabolism than [^{18}F]FESPA-RQ. Given the slower relative rates of metabolism of [^{18}F]SPA-RQ and [^{18}F]SPA-RQ-d_2 than [^{18}F]FESPA-RQ, one would expect better results in vivo in human studies with either [^{18}F]SPA-RQ or [^{18}F]SPA-RQ-d_2.

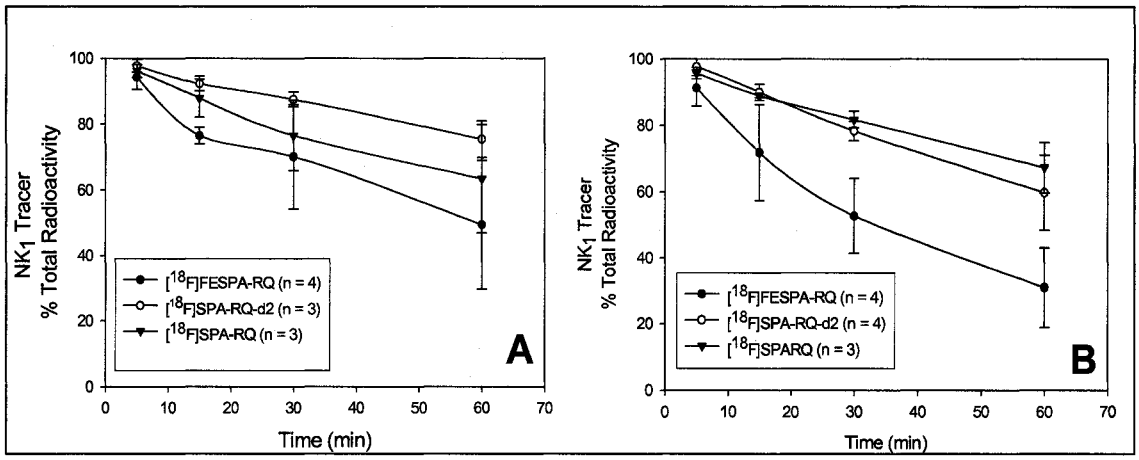

Figure 18. In vitro metabolism of [^{18}F]SPA-RQ, [^{18}F]SPA-RQ-d2, and [^{18}F]FESPA-RQ in rhesus monkey (A) and human (B) liver microsomes. Error bars represent standard deviation of percent total radioactivity for each time point.

The presence of free fluoride was evaluated in the in vitro metabolism samples as well, with the results shown in Figure 19. In this case, [^{18}F]F- was not the most dominant radiolabeled metabolite in these samples as was observed in the in vivo monkey plasma samples. There is no significant difference between all three tracers in the level of [^{18}F]F- in either species.

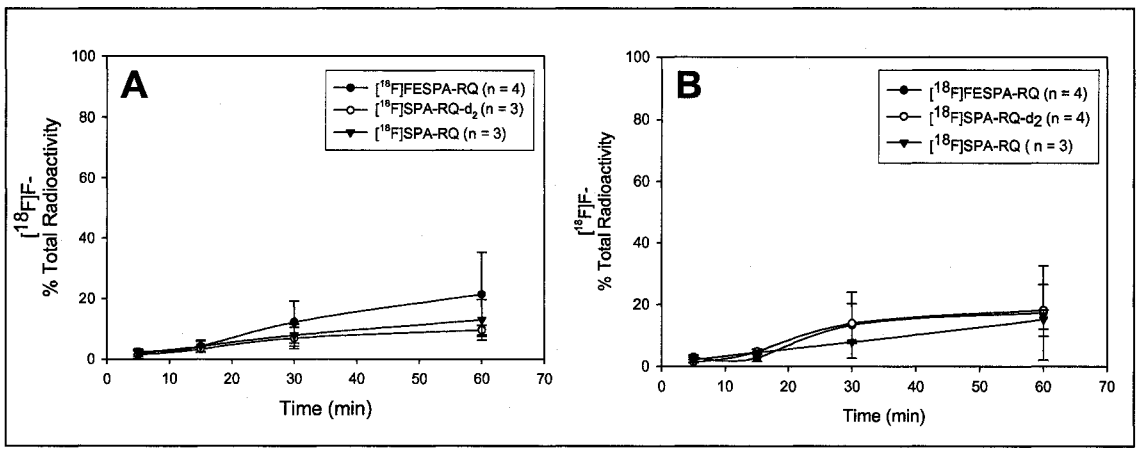

Figure 19. Presence of [^{18}F]F- in rhesus monkey and human liver microsome incubations with [^{18}F]SPA-RQ, [^{18}F]SPA-RQ-d$_2$, and [^{18}F]FESPA-RQ plotted as mean percent total radioactivity at each time point. Error bars are standard deviation of the measurement at each time point.

Unlike the in vivo studies, the majority of radioactivity over time in the in vitro samples was not due to [^{18}F]F-. After 60 min, the majority of the radioactivity was due to metabolite M3, which, based on its elution order on the HPLC chromatogram, was more polar than the parent compound and not likely to cross the blood-brain barrier. Representative chromatograms of each tracer in human and rhesus monkey liver microsomes are found in Figure 20. Although the presence of [^{18}F]F- was different in vitro than in vivo, the relative rates of metabolism of the three tracers better stability may be expected with [^{18}F]SPA-RQ or [^{18}F]SPA-RQ-d_2. Based on the results reported here, it is likely that either [^{18}F]SPA-RQ or [^{18}F]SPA-RQ-d_2 would have been chosen for use in human studies if the data had been available at the time of development. Since there was no significant difference in the metabolism of either [^{18}F]SPA-RQ or [^{18}F]SPA-RQ-d_2 and the presence of free fluoride was not significantly different, then the choice to use [^{18}F]SPA-RQ would have been supported by the data presented here.

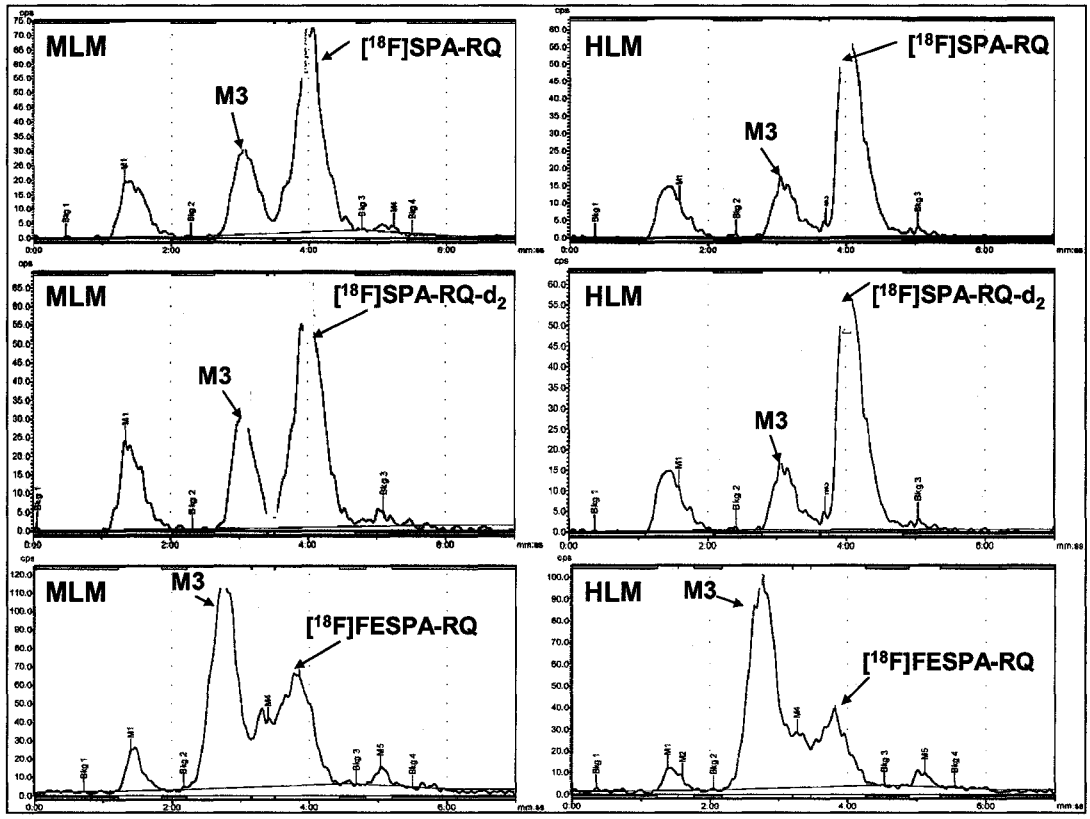

Figure 20. Representative radiochromatograms from the in vitro analysis of [^{18}F]SPA-RQ, [^{18}F]SPA-RQ-d_2, and [^{18}F]FESPA-RQ in rhesus monkey (MLM) and human (HLM) liver microsomes. All chromatograms are from samples obtained after 60 min incubation at 37°C.

5.3.3. Plasma Protein Binding

Protein binding of [^{18}F]SPA-RQ, [^{18}F]SPA-RQ-d_2, and [^{18}F]FESPA-RQ was evaluated in rhesus monkey and human plasma. The results are summarized in Figure 21. For all three tracers, there was slightly more tracer available in the free fraction of monkey plasma compared to human plasma. In both human and monkey plasma, there was slightly more [^{18}F]FESPA-RQ in the free fraction compared to [^{18}F]SPA-RQ and [^{18}F]SPA-RQ-d_2. For [^{18}F]FESPA-RQ, the free fraction was approximately 8% in human and 10% in monkey plasma. The free fraction for [^{18}F]SPA-RQ-d_2 was approximately

6% in human and 8% in monkey plasma and for [^{18}F]SPA-RQ, the free fraction was 4% in human and 5% in monkey. In this case, plasma protein binding was not a significant factor in the development of the tracers. The free fraction was high enough for penetration of all the tracers into the brain of rhesus monkeys as viewed from PET scans. The higher uptake of [^{18}F]SPA-RQ and [^{18}F]SPA-RQ-d_2 as compared to [^{18}F]FESPA-RQ could be more likely due to metabolism than plasma protein binding. Metabolism of [^{18}F]FESPA-RQ was slightly more rapid than [^{18}F]SPA-RQ and [^{18}F]SPA-RQ-d_2 so less parent tracer would be available for entry to the brain, thus resulting in the apparent lower brain uptake by PET.

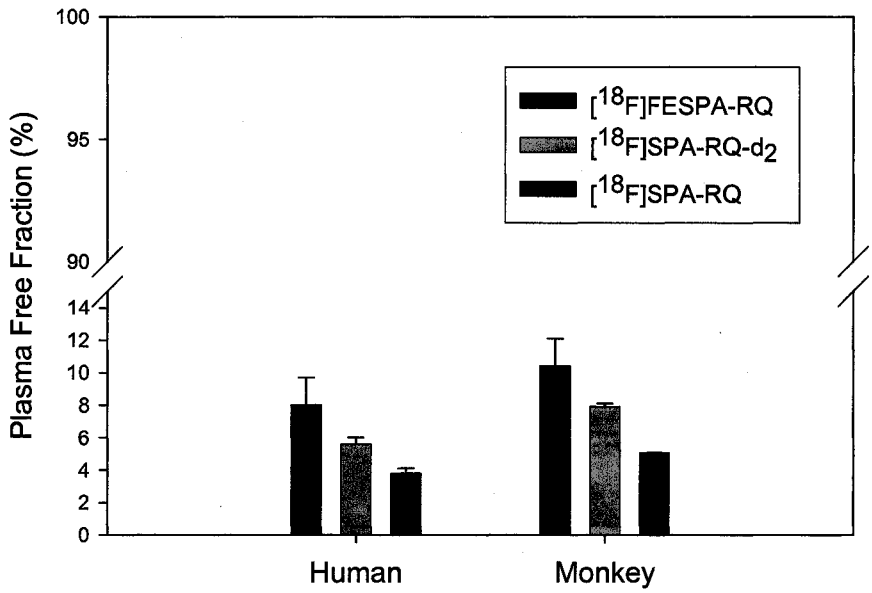

Figure 21. Free fraction (percent) of [^{18}F]SPA-RQ, [^{18}F]SPA-RQ-d_2 and [^{18}F]FESPA-RQ in rhesus monkey and human plasma corrected for nonspecific binding to the filters. Error bars represent the standard deviation of the measurements in each species (n =4).

5.4 [^{18}F]Tracer O – In Vitro Metabolism for Evaluation of Brain Uptake of Labeled Metabolite

[^{18}F]Tracer O is currently in development as a PET tracer for imaging a specific receptor in vivo in human clinical studies. During the development of the tracer, metabolism was evaluated in vivo in monkey plasma collected during PET imaging studies. Several labeled metabolites were observed over time in the monkey plasma samples. Figure 22 illustrates the metabolism of [^{18}F]Tracer O and the formation of two metabolites, M3 and M4, in monkey plasma. Data from one human subject is also included. The relative rate of metabolism of the tracer was very similar in monkey and human. It should be noted that data was only available for one human subject at the time of this report. In monkey plasma, the formation of metabolites M3 and M4 account for the majority of the radioactivity toward the end of a typical 90 min PET study.

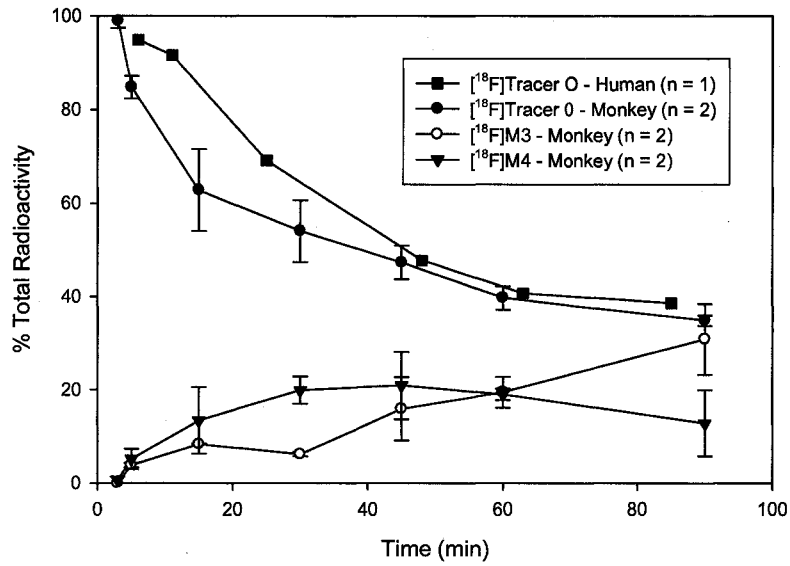

Figure 22. In vivo metabolism of [^{18}F]Tracer O in rhesus monkey and human plasma reported as percent total radioactivity. Formation of metabolites M3 and M4 are also included. Error bars are standard deviations for the measurements from two different monkeys.

Figure 23 illustrates chromatograms obtained from rhesus monkey plasma obtained 5 and 60 min after injection of [^{18}F]Tracer O and show the presence of the labeled metabolites. At 60 min, the presence of metabolites M3 and M4 were approximately equal to the levels of [^{18}F]Tracer O in plasma, but together account for more radioactivity than the parent tracer.

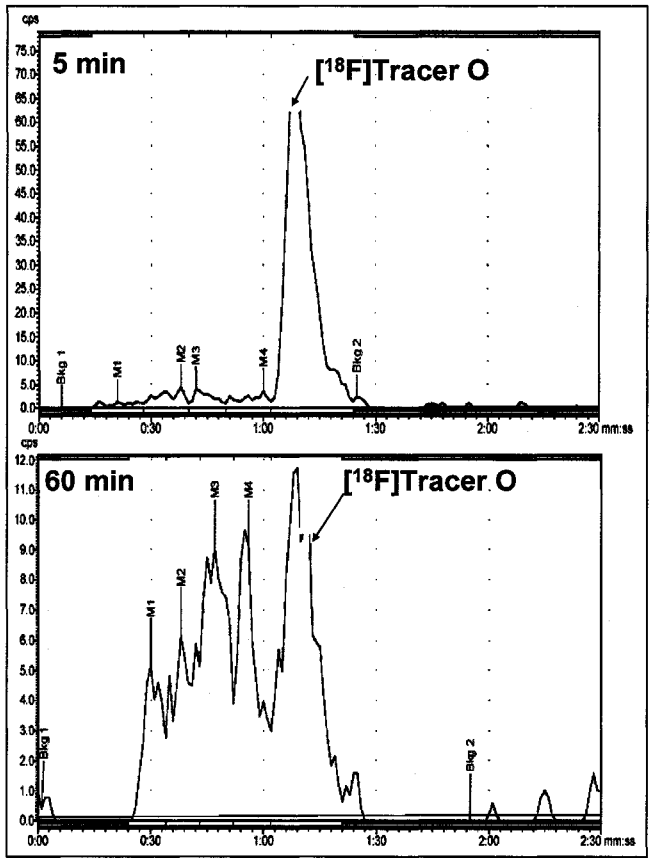

Figure 23. Representative radiochromatograms for the analysis of [^{18}F]Tracer O in rhesus monkey plasma. Samples were obtained 5 and 60 min after injection of tracer.

Prior to clinical studies with [^{18}F]Tracer O, in vitro metabolism studies were performed with human and rhesus monkey liver microsomes to determine whether the same metabolites were formed in humans as were observed in monkey plasma. The results are summarized in Figure 24 and show that in vitro metabolism in the two species

was very similar. The same metabolites were observed in monkey plasma samples as in the in vitro metabolism samples as determined by the matching retention times.

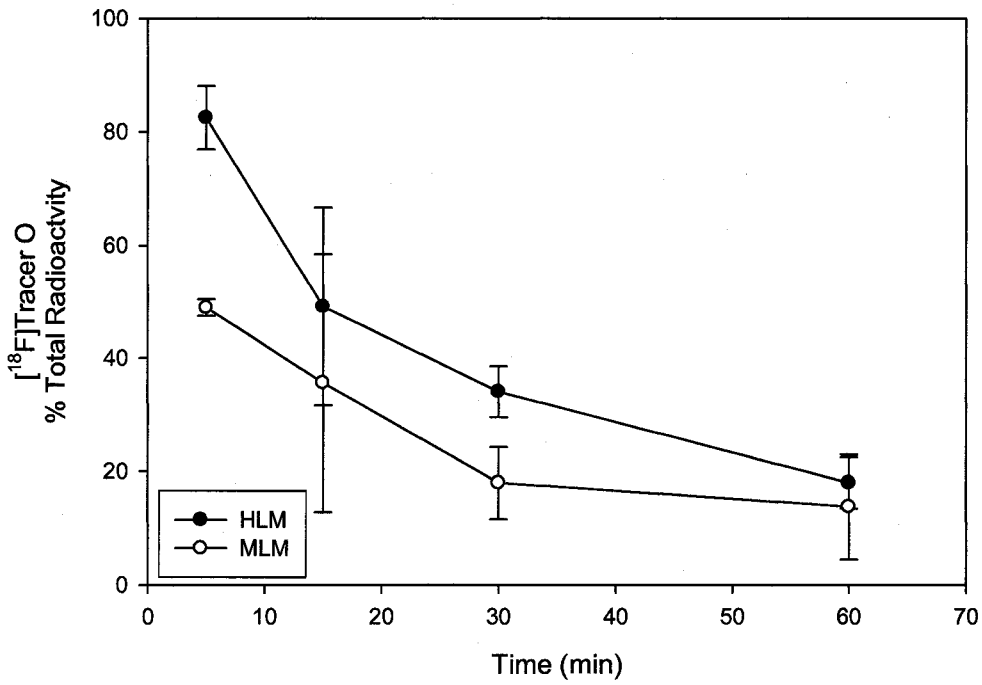

Figure 24. In vitro metabolism of [^{18}F]Tracer O in rhesus monkey (MLM) and human (HLM) liver microsomes. Error bars represent the standard deviation of multiple measurements (n = 3).

In order to determine the structures of the labeled metabolites, a set of in vitro samples were prepared that contained the addition of 1 μM of unlabeled Tracer O along with the labeled tracer. Data were collected using the radiochemical detector and the LC-MS/MS system. Precursor ion (Q1) scans were collected during the HPLC run to determine the molecular weight of the metabolites. Figure 25 illustrates the LC-MS/MS data obtained for the metabolites. As shown in the figure, the molecular ion (m/z 432.7) of the major labeled metabolite was likely due to hydroxylation. Based on the product ion scan of a 60 min incubation sample, the OH addition was determined to be on a

cylcohexyl ring which has four positions available for the placement of the OH group (data not shown). Based on the HPLC chromatogram (Figure 25C), there are multiple OH metabolites present in the in vitro metabolism samples.

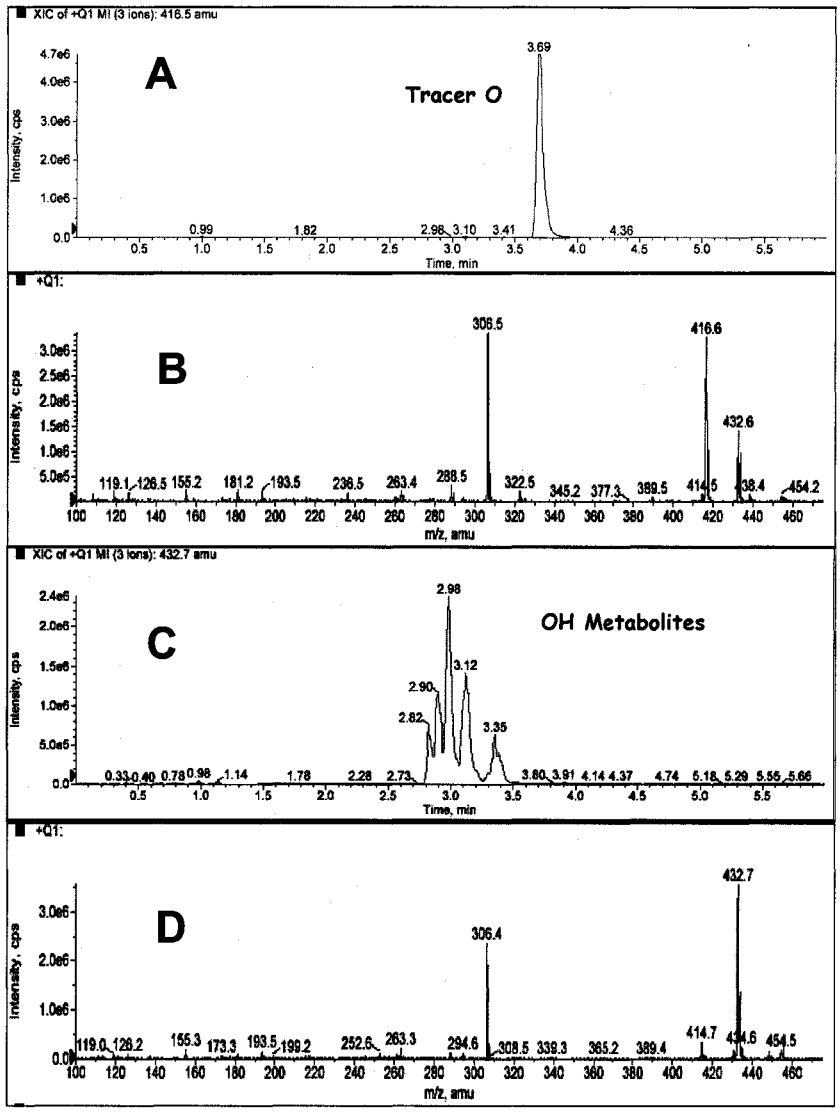

Figure 25. LC-MS chromatogram and mass spectra obtained after 60 min incubation of [^{18}F]Tracer O and 10 μM Tracer O in rhesus monkey liver microsomes.

A: Extracted ion chromatogram of Tracer O (m/z 416.6)
B: Mass spectrum for Tracer O, extracted from peak at retention time 3.69 min
C: Extracted ion chromatogram for OH metabolites of Tracer O (m/z 432.7)
D: Mass spectrum for OH metabolites, represented by peak at 3.12 min.

The possibility exists that the labeled metabolites could cross the blood-brain barrier and confound the PET signal of the parent tracer. The simplest way to determine whether the metabolites enter the brain would be to label precursors of the metabolites with ^{18}F and perform a PET scan. However, due to the number of possible metabolites, we were unable to obtain standard material of the metabolites for labeling. Thus, in vitro metabolism was used to attempt to make enough of the labeled metabolites to perform an in vivo study in a monkey. The in vitro metabolism procedures were scaled-up and run in parallel to prepare the labeled metabolites as previously described. Several conditions were evaluated to achieve an optimal level of labeled metabolites for injection in a monkey. Incubation conditions containing >10 mCi of parent tracer resulted in very little metabolism after 1 hour. Increasing the concentration of liver microsomes to 2 mg/mL resulted in almost complete metabolism of parent tracer. Following the cleanup and purification procedures, approximately 5 mCi of a sample containing [^{18}F]-labeled metabolites were injected into a rhesus monkey and PET studies performed. Two studies were performed in the same monkey on different days. In the first study, the monkey woke up after 30 min and the study was discontinued.

Figure 26 contains representative radiochromatograms obtained for the sample produced by incubation of the parent tracer resulting in labeled metabolites for injection and analysis by PET. The figure also contains a chromatogram for a plasma sample obtained 5 min after injection of the labeled metabolites, and a graph representing the presence of M4 in monkey plasma over time after injection of the labeled metabolites. Based on the chromatogram of the labeled metabolites, the majority of the injected sample contained a mixture of M3 and M4 (83% of total radioactivity). Based on mass

spectrometric data, M3 is likely a dihydroxylated metabolite and is less concentrated in the final incubation solution than M4. The early-eluting radioactive peak is due to a more polar metabolite that is not likely to cross the blood-brain barrier. The identity of [^{18}F]M4 was confirmed by mass spectrometry by detection of a molecular ion of m/z 432. Chromatographic retention time provided further confirmation of the labeled metabolite of interest. After injection, the labeled metabolite was relatively stable in plasma over time, with approximately 55% of the radioactivity due to [^{18}F]M4 after 60 min.

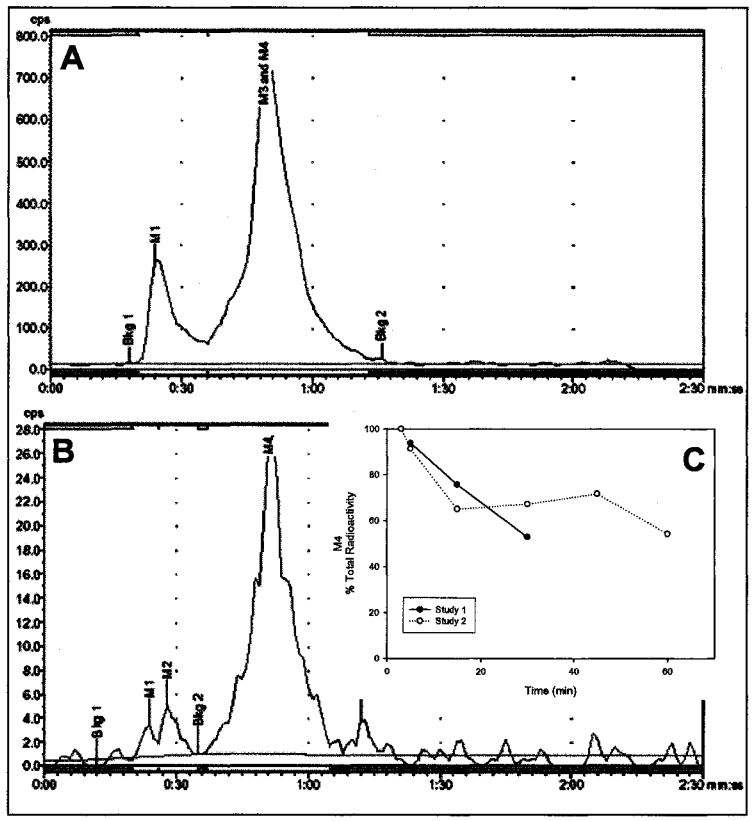

Figure 26. Representative radiochromatograms for the analysis of [^{18}F]-labeled metabolites injected during a rhesus monkey PET study.

A: Chromatogram obtained form the analysis of a sample of the [^{18}F]-labeled metabolites injected in a monkey for imaging by PET.
B: Chromatogram obtained from the analysis of a plasma sample obtained from a rhesus monkey 5 min after the injection of [^{18}F]-labeled metabolites.
C: Relative presence of [^{18}F]M4 over time in rhesus monkey plasma after injection of [^{18}F]-labeled metabolites.

Based on the results from the PET study, there was some uptake of the radiolabeled metabolites in the brain of the rhesus monkey studied with little washout. Figure 27 illustrates the graphical results, or time activity curve (TAC), obtained from the PET imaging study with the [^{18}F]-labeled metabolites. The results are plotted along with results obtained from a baseline imaging study performed with [^{18}F]Tracer O. Some uptake of the labeled metabolites was observed in the brain of the monkey studied, although significantly less than that of the parent tracer. Based on the results from the plasma analysis, the metabolites observed in the brain were likely [^{18}F]M4, or the hydroxylated metabolite of [^{18}F]Tracer O. Once in the brain, the labeled metabolites did not wash out quickly. It is unclear at this time whether the signal observed in the brain due to the metabolites is specific for the receptor of interest. Further studies using a blocking drug are needed to determine the specificity of the signal. These studies do illustrate the usefulness of a scaled-up in vitro metabolism incubation to produce labeled metabolites of a tracer that were not available as standard materials. Furthermore, LC-MS/MS coupled with a radiochemical detector was helpful in determining the structure of the labeled metabolite and confirming the structure of the metabolites prepared from the incubation.

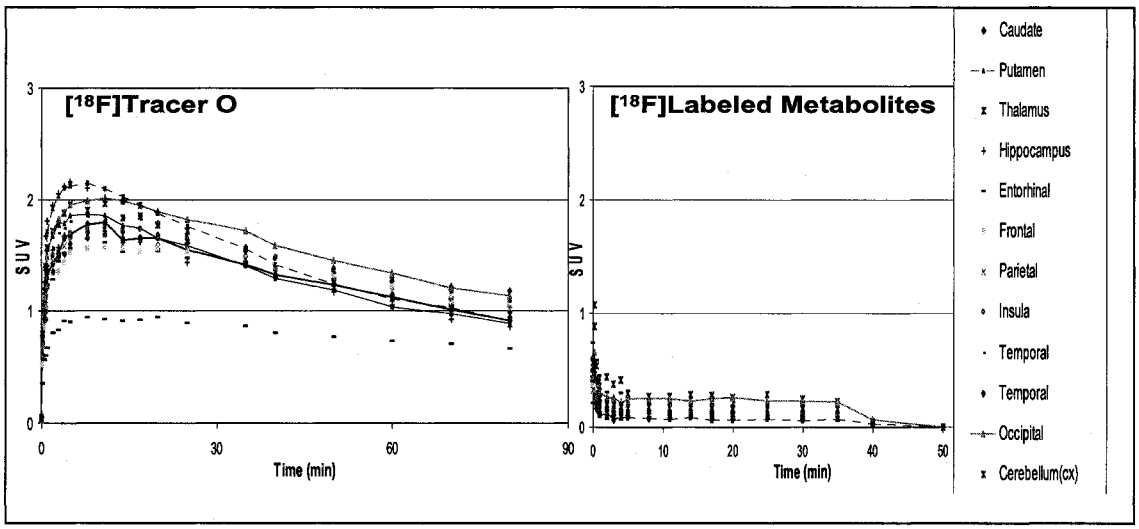

Figure 27. Uptake of [^{18}F]Tracer O and its labeled metabolites in various regions of the brain of a rhesus monkey. The scan was stopped at 35 min. SUV is the standardized uptake value which correlates dose injected, injection time, decay of the tracer, and monkey weight. Data courtesy of W. Eng, Imaging Research.

5.5 [^{18}F]Tracer MG

In vivo metabolism and plasma protein binding were applied to explain results observed in PET data after treatment with [^{18}F]Tracer MG and a blocking drug. Generally, when a blocking drug is administered prior to a tracer, the signal obtained for the tracer in vivo should be lower than when the tracer is administered alone. However, when the blocking drug for this program was administered prior to the tracer, the PET signal increased as compared to the baseline scan. To understand the cause for this result, several experiments were performed.

First, in vivo metabolism of the tracer was evaluated in two monkeys both in the presence of blocking drug and with tracer alone. The results are summarized in Figure 28. There was very little variability in the metabolism in both monkeys whether the tracer was administered alone or in the presence of the blocking drug. At 90 min post-injection

of tracer, approximately 20-25% of the total radioactivity was due to parent tracer. Based on these results, metabolism does not account for the changes observed in the PET imaging results for this tracer in the presence of the blocking drug. Thus, plasma protein binding was evaluated as a possible explanation for the increase in uptake of the tracer in the brain of the monkeys.

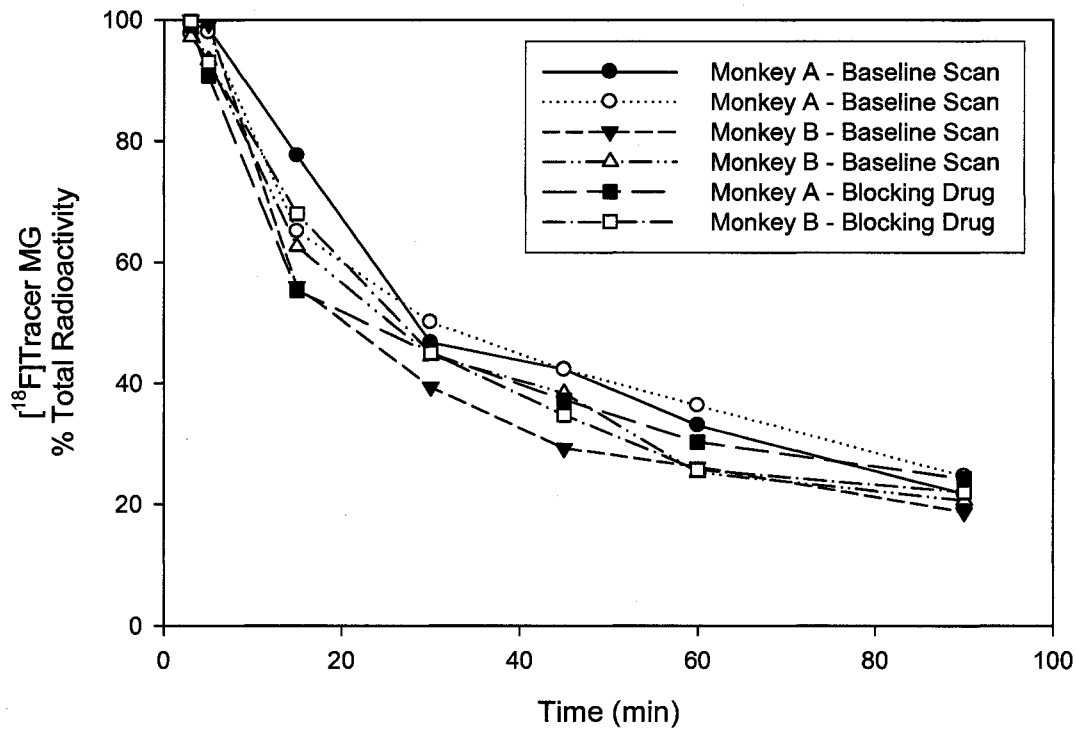

Figure 28. In vivo metabolism of [^{18}F]Tracer MG in rhesus monkey plasma with and without blocking drug reported as percent total radioactivity. Baseline scans were performed with approximately 5 mCi of tracer alone.

Monkey A Blocking Drug: 1.8 mpk bolus injection, 0.72 mpk/hr infusion for 1 hour, then ~5 mCi [^{18}F]Tracer MG.
Monkey B Blocking Drug: 0.9 mpk bolus injection, 0.36 mpk/hr infusion for 1 hour, then ~5 mCi [^{18}F]Tracer MG.

Plasma protein binding of the tracer was evaluated with and without blocking drug present using the same monkeys as the in vivo metabolism studies. For plasma protein binding studies, plasma was obtained from the monkeys prior to administration of the blocking drug and again at the end of drug infusion. Enough plasma was obtained so that replicate (n = 4) protein binding measurements could be performed. Labeled tracer was added to the plasma and incubated before using centrifuge filters to evaluate the levels of tracer in total plasma compared to that in the plasma free fraction. The results are summarized in Figure 29. In both monkeys, there was a difference in the level of plasma protein binding before the blocking drug was administered compared to 1 hour after the bolus+infusion. For Monkey A, free fraction was 25.3% ± 2.6% before blocking drug and 36.6% ± 3.4% after administration of the blocking drug. The change in free fraction was even more significant in Monkey B with a free fraction of 18.2% ± 1.2% before blocking drug and 39.0% ± 1.5% after treatment with the blocking drug. As shown by the model in Figure 1, the free fraction (C_f) of the tracer describes what is available for binding, either specifically or non-specifically, and can be estimated by plasma protein binding studies. The increased free fraction observed for [^{18}F]Tracer MG in the presence of the blocking drug serves as a very plausible explanation for the increased signal observed in the PET studies. The blocking drug may bind more readily to the same plasma proteins as the tracer, making the tracer more freely available for crossing the blood-brain barrier and ultimately increasing the signal observed in the PET scan. As a result of these studies and results from other PET imaging studies, development of tracers from a different structural class are currently being pursued to support this program.

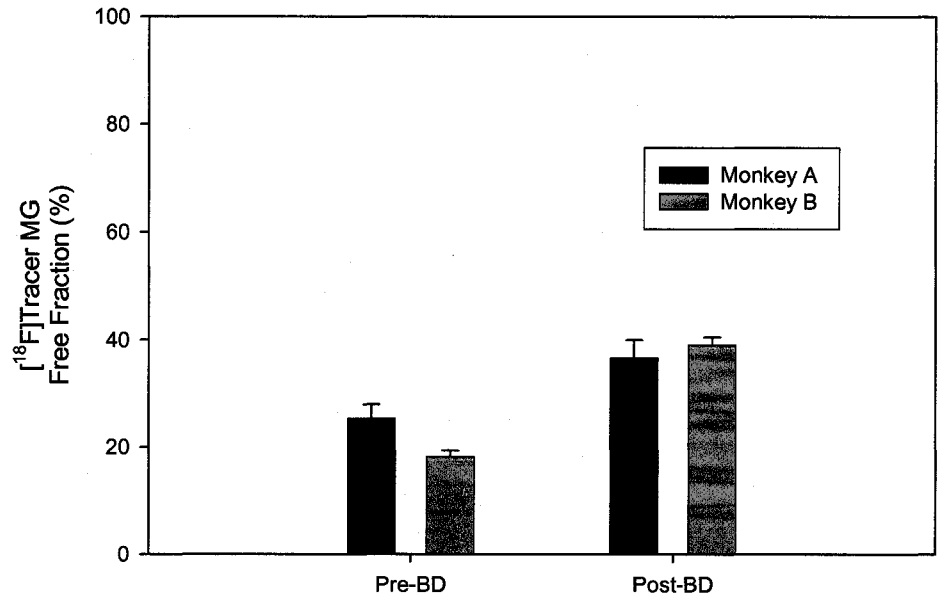

Figure 29. Plasma free fraction (percent) of [^{18}F]Tracer MG in rhesus monkey plasma before and after treatment with blocking drug (BD). N = 4 measurements per treatment.
Monkey A Blocking Drug: 1.8 mpk bolus injection, 0.72 mpk/hr infusion for 1 hour, then ~5 mCi [^{18}F]Tracer MG.
Monkey B Blocking Drug: 0.9 mpk bolus injection, 0.36 mpk/hr infusion for 1 hour, then ~5 mCi [^{18}F]Tracer MG.

6. Summary of Results

Analytical techniques were developed and optimized to allow for the rapid analysis and detection of radiolabeled PET tracers in animal plasma and in vitro metabolism samples. Given the short half-lives of commonly used PET tracers, analytical methods must be rapid and sensitive. The use of a monolithic column was investigated for the ability to rapidly analyze samples by HPLC with detection by a radiochemical detector and a mass spectrometer. Analyses utilizing the monolithic column were found to be rapid, with most run times completed within 2.5 min. This type of column was found to be extremely useful in conducting the in vitro metabolism studies. In the case of the AT_1

PET tracers, three species could be evaluated with 4 time points each, prepared in triplicate. Using the monolithic column, all of the samples were analyzed prior to radiochemical decay, including those studies with the ^{11}C tracer. This would not have been possible using a more traditional column with a slower flow rate and longer run time. In addition, the monolithic columns have a rod-shaped stationary phase which allows for the direct injection of plasma samples without clogging the column. The limiting factor in this case was whether the auto-injector could be rinsed sufficiently and in a timely manner to remove residual plasma from the injection needle or injection port. The rinse solvent was optimized to include a predominantly aqueous solution, and no problems were encountered with the injection of multiple samples. The use of the radiochemical detector in-line with the mass spectrometer allowed for the identification of metabolites when necessary, as well as confirmation of the structure of the radiolabeled tracer.

In vivo and in vitro metabolism and plasma protein binding studies were utilized to determine whether metabolism or level of tracer in the plasma free fraction may hinder the further development of novel PET tracers. In the case of mGluR5, in vivo metabolism was variable but parent tracer still remained during the length of a typical PET study. From the in vitro metabolism studies, the relative rate of metabolism in human liver microsomes was faster than in monkey liver microsomes. This result was the opposite of what was previously reported by Hamill et al. [35] where the study was conducted with higher concentrations of unlabeled tracer. In vitro and in vivo metabolism in monkey correlated well, so although the relative rate of in vitro metabolism was faster in human liver microsomes, there may still be enough parent tracer remaining at the end of a typical

PET study for [^{18}F]F-PEB to be successful in clinical imaging studies. Plasma protein binding was remarkably similar in both human and monkey. This result combined with the in vitro metabolism results along with uptake in monkey brain as observed by PET scans, indicates that this tracer may have a good probability of success in human subjects. Clinical trials with this tracer are currently under discussion.

For the AT_1 PET tracers, both metabolism and plasma protein binding were thought to be possible factors contributing to the failure of [^{11}C]L-159,884 in human clinical studies when dog imaging studies had been successful. Based on in vitro metabolism studies, there was very little difference between species in the metabolism of [^{11}C]L-159,884 and little difference between dog and human for [^{18}F]FMe-L-159,884-d_2. However, the relative rate of metabolism for [^{18}F]FMe-L-159,884-d_2 in dog and human was slower than for [^{11}C]L-159,884, indicating that if rapid metabolism was the cause of the failure of [^{11}C]L-159,884 in human studies, then [^{18}F]FMe-L-159,884-d_2 may have been a better tracer. In plasma protein binding studies, there was very little difference in plasma protein binding of the two tracers in the three species studied. However, there was an approximately 3-fold increase in the free fraction in dog plasma than in human for both tracers. Thus, even though there was a difference in the rate of metabolism between the two tracers, plasma protein binding may limit the use of [^{18}F]FMe-L-159,884-d_2 in human imaging studies. Furthermore, the procedures for determining plasma protein binding were optimized using the two AT_1 PET tracers. Pre-treating the centrifuge filters with unlabeled tracer prior to the addition of plasma samples limits the non-specific binding of the tracer to the filters. The use of protein-free plasma as a control sample, also allowed for correction for non-specific binding of the tracers.

Similar metabolism for the three NK_1 PET tracers studied was observed in vivo in monkeys with defluorination of the tracer being the major route of metabolism. Based on in vitro metabolism studies, the fastest metabolism in human liver microsomes was by [^{18}F]FESPA-RQ with very little difference between [^{18}F]SPA-RQ and [^{18}F]SPA-RQ-d_2. Defluorination of the tracers was not a significant route of metabolism for any of the NK_1 tracers in the in vitro metabolism experiments. [^{18}F]SPA-RQ has been used successfully in clinical imaging studies with some defluorination of the tracer observed. However, this has not hindered the use of this tracer in the clinic. In vitro studies were useful in comparing the relative rates of metabolism of the tracers in human and monkey and could contribute to the decision when multiple tracers are available for potential use in clinical studies. Protein binding appears to be less of an issue for the NK_1 tracers than metabolism. [^{18}F]FESPA-RQ had slightly higher levels in the free fraction of both human and monkey than the other two tracers. In this case, plasma protein binding may not have been a significant issue in the development of these PET tracers.

The methods that were developed and optimized for analysis of the mGluR5, AT_1, and NK_1 PET tracers were applied to two tracers currently in development. In the case of [^{18}F]Tracer O, LC-MS/MS was employed in conjunction with a radiochemical detector to identify the labeled metabolites of the tracer. Due to the number of possible structures for the labeled metabolites, no standard material was made available for labeling for use in a PET study. Thus, in vitro microsome incubations were scaled up and applied to the successful preparation of labeled metabolites of the tracer for injection and analysis in a monkey PET study. Based on PET study results, there was some uptake of the metabolites in the brain of the monkeys studied with little washout. Furthermore, the

same metabolites were formed in human liver microsomes as monkey liver microsomes as observed from the in vivo metabolism experiments. This is the first report of using in vitro metabolism to produce the labeled metabolites desired for study. Further work is required to determine whether the uptake seen in the monkey brain was specific. The tracer is currently being evaluated in human studies, and labeled metabolites of the tracer may need to be accounted for in the model used to characterize the behavior of the tracer in vivo.

The metabolism and plasma protein binding procedures were also applied to determine differences observed in PET data obtained in monkeys after injection of [^{18}F]Tracer MG and a blocking drug. Increased uptake of the tracer was observed in two different monkeys in the presence of a blocking drug. Based on the results of in vivo metabolism studies, metabolism was ruled out as the cause of the increased uptake of the tracer in the presence of the blocking drug. However, an increase in the free fraction of the tracer in the presence of the blocking drug was observed in plasma protein binding studies performed in plasma obtained from the monkeys before and after treatment with the blocking drug. Higher tracer in the free fraction could result in higher uptake in the brain. The results of these studies provided additional information to the program and development of [^{18}F]Tracer MG was discontinued.

Based on the results of these studies, metabolism and plasma protein binding can play a role in the successful development of a novel PET tracer. However, there are many factors that are not included in these studies that can not be accounted for, such as transport mechanisms. These methods and procedures serve to provide additional information to assist in the successful development of novel PET tracers. Additionally,

the methods and procedures reported here are currently regularly used during the development of novel PET tracers.

7. Conclusions

Rapid and sensitive techniques were developed and utilized for the analysis of several PET tracers in vivo in rhesus monkey plasma. The use of a monolithic column allowed for fast run times which, in turn, allowed for the analysis of multiple sets of in vitro metabolism samples. Methods were also optimized for the rapid analysis of plasma protein binding of PET tracers. The methods were optimized using PET tracers in various stages of development, one successfully used in human clinical trials, one failed in human studies, and one not yet administered in human studies. The methods were used as a retrospective means to determine whether in vivo and in vitro metabolism and plasma protein binding can be used to aid in the decision of whether to move a tracer to clinical study. The methods were then applied to two tracers currently under development at Merck Research Laboratories (MRL). The methods and procedures were useful in providing information for the further development of the two tracers. One major implication of this work is that these procedures can and are routinely used in the development and optimization of novel PET tracers.

GLOSSARY OF ABREVIATIONS

[^{18}F]F-PEB – [^{18}F]3-fluoro-5-[(pyridine-3-yl)ethynyl]benzonitrile

[^{11}C]L-159,884 – [^{11}C]*N*-[[4'[(2-ethyl-5,7-dimethyl-3H-imidazol[4,5-b]pyridine-3-yl)methyl][1,1'biphenyl]-2-yl]sulfonyl]-4-methoxybenzamide

[^{18}F]FMe-L-159,884-d2 - [^{18}F]*N*-[[4'[(2-ethyl-5,7-dimethyl-3H-imidazol[4,5-b]pyridine-3-yl)methyl][1,1'biphenyl]-2-yl]sulfonyl]-4- fluorodideuteromethoxybenzamide

[^{18}F]SPA-RQ – [^{18}F][2-fluoromethoxy-5-(5-trifluoromethyl-tetrazol-1-yl)-benzyl]-([2S,3S])-2-phenyl-piperidin-3-yl)amine

[^{18}F]SPA-RQ-d_2 – [^{18}F][2-fluorodideuteromethoxy-5-(5-trifluoromethyl-tetrazol-1-yl)-benzyl]-([2S,3S])-2-phenyl-piperidin-3-yl)amine

[^{18}F]FESPA-RQ – [^{18}F][2-fluoroethoxy-5-(5-trifluoromethyl-tetrazol-1-yl)-benzyl]-([2S,3S])-2-phenyl-piperidin-3-yl)amine

BBB – Blood-brain barrier

mGluR5 – Metabotropic glutamate subtype 5 receptor

AT_1 – Angiotensin 1 receptor

NK_1 – Neurokinin 1 receptor

PET – Positron emission tomography

LC-MS/MS – Liquid chromatography-mass spectrometry/mass spectrometry

HPLC - High performance liquid chromatography

TLC – Thin layer chromatography

REFERENCES

[1] Riffel, K.A., Groff, M.A., Wenning, L., Song, H., Lo, M.-W. (2005) Fully automated liquid-liquid extraction for the determination of a novel insulin sensitizer in human plasma by heated nebulizer and turbo ionspray liquid chromatography-tandem mass spectrometry. *J. Chrom. B.* 819, 293-300.

[2] Riffel, K.A., Song, H., Gu, X., Yan, K., Lo, M.-W. (2000) Simultaneous determination of a novel thrombin inhibitor and its two metabolites in human plasma by liquid chromatography/tandem mass spectrometry. *J. Pharm. Biomed. Anal.* 23, 607-616.

[3] Groff, M., Riffel, K., Song, H., Lo, M.W. (2006) Stabilization and determination of a PPAR agonist in human urine using automated 96-well liquid-liquid extraction and liquid chromatography/tandem mass spectrometry. *J. Chrom. B.* 842, 122-130.

[4] Cherry, S. R. (2001). Fundamentals of positron emission tomography and application in preclinical drug development. *J. Clin. Pharmacol.* 41, 482-491.

[5] Årstad, E., Platzer, S., Berthele, A., Pilowsky, L.S., Luthra, S.K., Wester, H.-J., Henrikson, G. (2006). Toward NR2B receptor selective imaging agents for PET – synthesis and evaluation of *N*-[^{11}C]-(2-methoxy)benzyl(E)-styrene-, 2-naphthyl-, 4-trifluoromethoxyphenylamidine. *Biorg. Med. Chem.* 14, 6307-6313.

[6] Fischman, A.J., Alpert, N.M., Babich, J.W., Rubin, R.H.. (1997). The role of positron emission tomography in pharmacokinetic analysis. *Drug Metab. Rev.* 29(4), 923.

[7] Phelps, M.E. (1991) PET: A biological imaging techniques. *Neurochem. Res.* 16(9), 929.

[8] Bergström, M., Fasth, K.-J., Kilpatrick, G., Ward, P., Cable, K.M., Wipperman, M.D., Sutherland, D.R., Långström, B. (2000). Brain uptake and receptor binding of two [^{11}C]labeled selective high affinity NK1-antagonists, GR203040 and GR 205171 – PET studies in rhesus monkey. *Neuropharm.* 39, 664.

[9] Lammertsma, A. (2002). Radioligand studies: imaging and quantitative analysis. *European Neuropsychopharmacology.* 12, 513-516.

[10] Schmidt, K.C., Turkheimer, F.E. (2002). Kinetic modeling in positron emission tomography. *Q. J. Nucl. Med.* 46, 70-85.

[11] Cummings, P., Yokoi, F., Chen, A., Deep, P., Dagher, A., Reutens, D., Kapczinski, F., Wong, D.F., Gjedde, A. (1999). Pharmacokinetics of radiotracers in human plasma during positron emission tomography. *Synapse*. 34, 124-134.

[12] Wilson, A.A., McCormick, P., Kapur, S., Willeit, M., Garcia, A., Hussey, D., Houle, S., Seeman, P., Ginovart, N. (2006). Radiosynthesis and evaluation of [^{11}C]-(+)-4-propyl-3,4,4a,5,6,10b-hexahydro-2H-naphthol[1,2-b][1,4]oxazin-9-ol as a potential radiotracer for in vivo imaging of the dopamine D2 high-affinity state with positron emission tomography. *J. Med. Chem.* 48, 4153-4160.

[13] Kwong, T.C. (1985). Free drug measurements: methodology and clinical significance. *Clinical Chima Acta.* 151, 193-216.

[14] Lee, S-Y., Choe, Y.S., Kim, D.H., Park, B-K., Kim, S.E., Choi, Y., Lee, K-H., Lee, J., Kim, B-T. (2001) A simple and efficient in vitro method for metabolism studies of radiotracers. *Nucl. Med. Biol.* 28, 391-395.

[15] Ryu, E.K., Choe, Y.S., Kim, D.H., Ko, B.-H., Choi, Y., Lee, K.-H., Kim, B.-T. (2006). In vitro metabolism studies of ^{18}F-labeled 1-phenylpiperazine using mouse liver S9 fraction. *Nucl. Med. Biol.* 33, 165-172.

[16] Lavén, M., Markides, K., Långström, B. (2004) Analysis of microsomal metabolic stability using high-flow-rate extraction coupled to capillary liquid chromatography–mass spectrometry. *J. Chrom. B.* 806, 119-126.

[17] Levêque, P., de Hoffmann, E., Labar, D., Gallez, B. (2001) Assessment of [^{18}F]fluoroethylflumazenil metabolites using high performance liquid chromatography and tandem mass spectrometry. *J. Chrom. B.* 754, 35-44.

[18] Lavén, M., Itsenko, O., Markides, K., Långström, B. (2006) Determination of metabolic stability of positron emission tomography tracers by LC–MS/MS: An example in WAY-100635 and two analogues. *J. Pharm. Biomed. Anal.* 40, 943-951.

[19] Hilton, J., Yokoi, F., Dannals, R.F., Ravert, H.T., Szabo, Z., Wong, D.F. (2000) Column-switching HPLC for the analysis of plasma in PET imaging studies. *Nucl. Med. Biol.* 27, 627-630.

[20] Gillings, N.C., Bender, D., Falborg, L., Marthi, K., Munk, O.L., Cumming, P. (2001). Kinetics of the metabolism of four PET radioligands in living minipigs. *Nucl. Med. Biol.* 28, 97-104.

[21] Zea-Ponce, Y., Larulelle, M. (1999) Protein precipitation: an expedient procedure for the routine analysis of the plasma metabolites of [^{123}I]IZBM. *Nucl. Med. Biol.* 26, 811-814.

[22] Greuter, H.N.J.M., van Ophemert, P.L.B., Luurtsema, G., van Berckel, B.N.M., Franssen, E.J.F., Windhorst, B.D., Lammertsma, A.A. (2000) Optimizing an online SPE–HPLC method for analysis of (*R*)-[^{11}C]1-(2-chlorophenyl)-*N*-methyl-*N*-(1-methylpropyl)-3-isoquinolinecarboxamide [(*R*)-[^{11}C]PK11195] and its metabolites in humans. *Nucl. Med. Biol.* 32, 307-312.

[23] Ma, Y., Kiesewetter, D.O., Lang, L., Der, M., Huang, B., Carson, R.E., Eckelman, W.C. (2003) Determination of [^{18}F]FCWAY, [^{18}F]FP-TZTP, and their metabolites in plasma using rapid and efficient liquid-liquid and solid phase extractions. *Nucl. Med. Biol.* 30, 233-240.

[24] Lindner, K.-J., Hartvig, P., Åkesson, C., Tyrefors, N., Sundin, A., Långström, B. (1996) Analysis of L-[methyl-^{11}C]methionine and metabolites in human plasma by an automated solid-phase extraction and a high-performance liquid chromatographic procedure. *J. Chrom. B.* 679,13-19.

[25] Jacobson, G.B., Moulder, R., Lu, L., Bergström, M., Markides, K.E., Långström, B. (1997) Supercritical Fluid Extraction of ^{11}C-Labeled Metabolites in Tissue Using Supercritical Ammonia. *Anal. Chem.* 69, 275-280.

[26] Mahar Doan, K.M., Wring, S.A., Shampine, L.J., Jordan, K.H., Bishop, J.P., Kratz, J., Yang, E., Serabjit-Singh, C., Adkison, K.K., Polli, J.W. (2004). Steady-state brain concentrations of antihistamines in rats. *Pharmacology.* 72, 92-98.

[27] Parepally, J.M.R., Mandula, H., Smith, Q.R. (2006) Brain uptake of nonsteroidal anti-inflammatory drugs: ibuprofen, flurbiprofen, and indomethacin. *Pharm Res.* 23(5), 873-881.

[28] van Waarde, A., Visser, T.J., Posthumus, H., Elsinga, P.H., Anthonio, R.L., van Loenen-Weemaes, A-M.A., Visser, G.M., Beaufort-Krol, G.C.M., Paans, A.M.J., Vaalburg, W. (1996) Quantification of the β-adrenoceptor ligand *S*-1'-[^{18}F]fluorocarazolol in plasma of humans, rats and sheep. *J. Chrom. B.* 678, 253-260.

[29] Santens, P., De Vos, F., Boudenm D., Slegers, G., Lemahieu, I., Boon, P., de Reuck, J. (1999). The pharmacokinetics of [^{11}C]methoxynorchloroprogabidic acid, a potential PET tracer for GABA receptors in the brain. *Nucl. Med. Biol.* 26, 323-325.

[30] Hume, S.P., Hirani, E., Opacka-Juffry, J., Osman, S., Myers, R., Gunn, R.N., McCarron, J.A., Clark, R.D., Melichar, J., Nutt, D.J., Pike, V.W. (2000) Evaluation of [O-methyl-^{11}C]RS-15385-197 as a positron emission tomography radioligand for central α_2-adrenoreceptors. *Eur. H. Nucl. Med.* 27, 475-484.

[31] Mankoff, D.A., Tewson, T.J., Eary, J.F. (1997) Analysis of blood clearance and labeled metabolites for the estrogen receptor tracer [F-18]-16α-fluoroestradiol (FES). *Nucl. Med. Biol.* 24, 341-348.

[32] Yasuno, F., Zoghbi, S.S., McCarron, J.A., Hong, J., Ichise, M., Brown, A.K., Gladding, R.L., Bacher, J.D., Pike, V.W., Innis, R.B. (2006). Quantification of serotonin 5-HT1A receptors in monkey brains with [^{11}C](R)-(-)-RWAY. *Synapse.* 60(7), 510-520.

[33] Obach, R.S. (2001) The prediction of human clearance from hepatic microsomal metabolism data. *Curr. Opin. Drug Disc. Dev.* 4, 36-44.

[34] Hamill, T.G., Krause, S., Ryan, C., Bonnefus, C., Govek, S., Seiders, T.J., Cosford, N.D.P., Roppe, J., Kamenecka, T., Patel, S., Gibson, R.E., Sanabria, S. , Riffel, K., Eng, W., King, C., Yang, X., Green, M.D., O'Malley, S.S., Hargreaves, R., Burns, H.D. (2005) Synthesis, characterization, and first successful monkey imaging studies of metabotropic glutamate receptor subtype 5 (mGluR5) PET radiotracers. *Synapse.* 56, 205-216.

[35] Mathews, W.B., Yoo, S-E., Lee, S.-H., Sceffel. U., Rauseo, P.A., Zober, Ta.G., Gocco, G., Sandberg, K., Ravert, H.T., Dannals, R.F., Szabo, Z. (2004). A novel radioligand for the AT_1 angiotensin receptor with PET. *Nucl. Med. Biol.* 31, 571-574.

[36] Hargreaves, R. (2002) Imaging Substance P receptors (NK_1) in the living human brain using positron emission tomography. *J. Clin Psych.* 63 (suppl 11), 18.

[37] Bergström, M., Hargreaves, R., Burns, H.D., Goldberg, M., Sciberras, D., Reines, S., Petty, K.J., Ögren, M., Antoni, G., Långström, B., Eskola, O., Scheinin, M., Solin, O., Majumdar, A., Constanzer, M., Battisti, W.P., Bradstreet, T.E., Gargano, C., Hietala, J. (2004). Human positron emission tomography studies of brain neurokinin 1 receptor occupancy by aprepitant. *Biol. Psych.* 55, 1007.

[38] Hietala, J., Nyman, M.J., Eskola, O., Lakso, A., Grönroos, T., Oikonen, V., Bergman, J., Haaparanta, M., Forsback, S., Marjamäki, P., Lehikoinen, P., Goldberg, M., Burns, D., Hamill, T., Eng, W., Coimbra, A., Hargreaves, R., Solin, O. (2005) Visualization and quantification of neurokinin-1 (NK_1) receptors in the human brain. *Mol. Imaging Biol.* 7. 262-272.

[39] Nyman, M.J., Eskola, O., Kajander, J., Vahlberg, T., Sanabria, S., Burns, D., Hargreaves, R., Solin, O., Hietala, J. (2006) Gender and age affect NK_1 receptors in the human brain – a positron emission tomography study with [^{18}F]SPA-RQ. *Int. J. Neuropsyhcopharmacol.* 30, 1-11.

[40] Yu, M., Tueckmantel, W., Wang, X., Zhu, A., Kozikowski, A.P., Brownell, A.-L. (2005). Methoxyphenylethynyl, methoxypyridylethynyl and phenylethynyl derivatives of pyridine: synthesis, radiolabeling and evaluation of new PET ligands for metabotropic glutamate subtype 5 receptors. *Nucl. Med. Biol.* 32, 631-640.

[41] Kokic, M., Honer, M., Ametamey, S.M., Gasparini, F., Andres, H., Bischoff, S., Flor, P.J., Heinrich, M., Vranesi, I., Spooren, W., Kuhn, R., Schubiger, P.A. (2001). Radiolabeling and in vivo evaluation of 11C]-M-MPEP as a PET radioligand for the metabotropic glutamate receptor 5 (mGluR5). *J. Labeled Compd. Radiopharm.* 44 (Suppl 1), S231-S232.

[42] Musachio, J.L., Ghose, S., Toyama, H., Kozikowski, A.P., Klaess, T., Mukhopadhyaya, J.K., Ichise, M., Hong, J., Zoghbi, S., Liow, J.S. Innis, R.B., Pike, V.W. (2003) Two potential mGluR5 PET radioligands, [^{11}C]M-MPEP and [^{11}C]methoxy-PEPy – synthesis and initial PET evaluation in rats and monkeys in vivo. *Mol. Imag. Biol.* 5, 168.

[43] Ametamey, S.M., Kessler, L., Honer, M., Auberson, Y., Gasparini, F., Schubiger, P.A. (2003) Synthesis and evaluation of [11C]M-FPEP as a PET ligand for imaging the metabotropic glutamate receptor subtype 5 (mGluR5). *J. Labeled Compd. Radiopharm.* 46 (Suppl 1), S188.

[44] Hamill, T.G., Seiders, T.J., Krause, S., Ryan, C., Sanabria, S., Gibson, R.E., Patel, S., Cosford, N., Roppe, J., Yang, J., King, C., Hargreaves, R.J., Burns, H.D. (2003). The synthesis and characterization of mGluR5 receptor PET ligands. *J. Labelled Compd. Radiopharm.* 46 (Suppl 1), S75.

[45] Krause, S.M., Hamill, T.G., Seiders, T.J., Ryan, C., Sanabria, S., Gibson, R.E., Patel, S., Cosford, N.D., Roppe, J.R., Hargreaves, R.J., Burns, H.D. (2003) In vivo characterizations of PET ligands for the mGluR5 receptor in rhesus monkey. *Mol. Imag. Biol.* 5, 166.

[46] Ametamey, S.M. Kessler, L.J., Honer, M., Wyss, M.T., Buck, A., Hintermann, S., Auberson, Y.P., Gasparini, F., Schubiger, P.A. (2006) Radiosynthesis and preclinical evaluation of [11C]ABP688 as a probe for imaging metabotropic glutamate receptor subtype 5. *J. Nucl. Med.* 47(40), 698-705.

[47] Hsieh, Y., Wang, G., Wang, Y., Chackalamannil, S., Korfmacher, W.A. (2003) Direct plasma analysis of drug compounds using monolithic column liquid chromatography and tandem mass spectrometry. Anal. Chem. 75(8), 1812.

[48] Barbarin N., Mawhinney, D.B., Black, R., Henion, J. (2002). High-throughput selected reaction monitoring liquid chromatography-mass spectrometry determination of methylphenidate and its major metabolite, rialinic acid, in rat plasma employing monolithic columns. *J. Chrom. B.* 783, 73.

[49] Hamill, T.G., Burns, H.D., Dannals, R.F., Mathews, W.B., Musachio, J.L., Ravert, H.T., Naylor, E.M. (1996). Development of [^{11}C]L-159,884: A radiolabeled, nonpeptide angiotensin II antagonist that is useful for angiotensin II, AT_1 receptor imaging. *Appl. Radiat. Isot.* 47(2), 211.

[50] Kim, S.E., Scheffel, U., Szabo. Z., Burns, H.D., Gibson, R.E., Ravert, H.T., Mathews, W.B., Hamill, T.G., Dannals, R.F. (1996) In vivo labeling of angiotensin II receptors with a carbon-11-labeled selective nonpeptide antagonist. *J. Nucl. Med.* 37, 307-311.

[51] Szabo, Z., Kao, P.F., Burns, H.D., Gibson, R.E., Hamill, T.G., Ravert, H.T., Kim, S.E., Mathews, W.B., Musachio, J.L., Scheffel, U., Dannals, R.F. (1998). Investigation of angiotensin II/AT_1 receptors with Carbon-11-L-159,884: a selective AT_1 antagonist. *J. Nucl. Med.* 39, 1209.

[52] Szabo, Z., Speth, R.C., Brown, P.R., Kerenyl, L., Kao, P.F., Mathews, W.B., Ravert, H.T., Hilton, J., Rauseo, P., Dannals, R.F., Zheng, W., Lee, S., Sandberg, K., (2001). Use of positron emission tomography to study AT_1 receptor regulation in vivo. *J. Am. Soc. Nephrol.* 12, 1350.

[53] Owonikoko, T.K., Fabucci, M.E., Brown, P.R., Nisar, N., Hilton, J., Mathews, W.B., Ravert, H.T., Rauseo, P., Sandberg, K., Dannals, R.F., Szabo, Z. (2004) In vivo investigation of estrogen regulation of adrenal and renal angiotensin (AT1) receptor expression by PET. *J. Nucl. Med.* 45(1), 94-100.

[54] Zober, T.G., Mathews, W.B., Seckin, E., Yoo, S., Hilton, J., Xia, J., Sandberg, K., Ravert, H.T., Dannals, R.F., Szabo, Z. (2006). PET imaging of the AT_1 receptor with [^{11} C]KR31173. Nucl. Med. Biol. 33, 5-13.

[55] Rupniak, N.M., Kramer, M.S. (1999). Discovery of the anti-depressant and anti-emetic efficacy of substance P receptor (NK_1) antagonists. *Trends in Pharm. Sci.* 20, 485.

[56] Del Rosario, R.B., Mangner, T.J., Gildersleeve, D.L., Shreve, P.D., Wieland, D.M., Lowe, J.A., Drozda, S.E., Snider, R.M. (1993). Synthesis of a nonpeptide carbon-11 labeled substance P antagonist for PET studies. *Nucl. Med. Biol.* 20(4), 545.

[57] Livni, E., Babich, J.W., Desai, M.C., Godek, D.M., Wilkinson, R.A., Rubin, R. H., Fischman, A.J. (1995) Synthesis of a ^{11}C-labeled NK_1 receptor ligand for PET studies. *Nucl. Med. Biol.* 22(1), 31.

[58] Michelgård, Å., Appel, L., Pissiota, A., Frans, Ö., Langström, B., Bergström. M, Fredrikson, M. (2006). Symptom provocation in specific phobias affects the substance P neurokinin-1 receptor system. *Biol. Psychiatry.* In press.

[59] Bender, D., Olsen, A.K., Marthi, M.K., Smith, D.F., Cumming, P. (2004). PET evaluation of the uptake of *N*-[^{11}C]-methyl CP-643,501, and NK_1 receptor antagonist, in the living porcine brain. *Nucl. Med. Biol.* 31, 699.

[60] Gao, M., Mock, B.H., Hutchins, G.D., Zheng, Q.-H. (2005). Synthesis and initial PET imaging of new potential NK1 receptor radioligands 1-[2-(3,5-bis-trifluoromehtyl-benzyloxy)-1-phenyl-ethyl]-4-[^{11}C]methyl-piperazine and {4-[2-(3,5-bis-trifluoromethyl-benzyloxy)-1-phenyl-ethyl]piperazine-1-yl}acetic acid [^{11}C]methyl ester. *Nucl. Med. Biol.* 32, 543-552.

[61] Solin, O., Eskola, O., Hamill, T.G., Bergman, J., Lehikoinen, P., Grönroos, T., Forsback, S., Haaparanta, M., Viljanen, T., Ryan, C., Gibson, R., Kieczykowski., G., Hietala, J., Hargreaves, R., Burns, H.D. (2004). Synthesis and characterization of a potent, selective, radiolabeled substance-P antagonist for NK_1 receptor quantitation: ([^{18}F]SPA-RQ). *Mol. Imaging Biol.* 6(6), 373.

[62] Keller, M., Montgomery, S., Ball, W., Morrison, M., Snavely, D., Liu, G., Hargreaves, R., Hietala, J., Lines, C., Beebe, K., Reines, S. (2006). Lack of efficacy of the substance P (neurokinin$_1$ receptor) antagonist aprepitant in the treatment of major depressive disorder. *Biol. Psychiatry.* 59, 216-223.

[63] Zoghbi, S.S., Shetty, H.U., Ichise, M. Fujita, M., Imaizumi, M. Liow, J.S., Shah, J., Musachio, J.L., Pike, V.W., Innis, R.B. (2006). PET imaging of the dopamine transporter with 18F-FECNT: a polar radiometabolite confounds brain radioligand measurements. *J. Nucl. Med.* 47(3), 520-527

[64] Staley, J.K., Van Dyck, C.H., Tan. P.-Z., Tikriti, M.A., Ramsby, Q., Klump, H., Ng, C., Garg, P., Soufer, R., Baldwin, R.M., Innins. R.B. (2001). Comparison of [^{18}F]altanserin and [^{18}F]deuteroaltanserin for PET imaging of serotonin2A receptors in baboon brain: pharmacological studies. *Nucl. Med. Biol.* 28, 271-279.

[65] Kim, K.-H., Isin, E.M., Yun, C.-H., Kim, D.-H., Guengerich, F.P. (2006). Kinetic deuterium isotope effects for 7-alkoxycoumarin *O*-dealkylation reactions catalyzed by human cytochromes P450 and in liver microsomes. Rate-limiting C-H bond breaking in cytochrome P450 1A2 substrate oxidation. *FEBS.* 273, 2223-2231.

[66] Fowler, J.S., Wolf, A.P., MacGregor, R.R., Dewey, S.L., Logan, J., Schyler, D.J., Langstrom, B. (1988). Mechanistic positron emission tomography studies: demonstration of a deuterium isotope effect in the monoamine oxidase-catalyzed binding of [^{11}C]L-deprenyl in living baboon brain. *J. Neurochem.*51(5), 1524-1534.

[67] Fowler, J.S., Wang, G.-J., Logan, J., Xie, S., Volkow, N.D., MacGregor, R.R., Schyler, D.J., Pappas, N., Alexoff, D.L., Patlak, C., Wolf, A.P. (1995). Selective reduction of radiotracer trapping by deuterium substitution: comparison of carbon-

11-L-deprenyl and carbon-11-L-deprenyl-D2 for MAO B mapping. *J. Nucl. Med.* 36(7), 1255-1262.

[68] Ding, Y.-S., Fowler, J.S., Gatley, J., Logan, J., Volkow, N.D., Shea, C. (1995). Mechanistic positron emission tomography studies of 6-[^{18}F]fluorodopa in living baboon heart: selective imaging and control of radiotracer metabolism using deuterium isotope effect. *J. Neurochem.* 65(2), 682-690.

[69] Zhang. M.-R., Maeda, J., Ogawa, M., Noguchi, J., Ito, T., Yoshida, Y., Okauchi, T., Obayashi, S., Suhara, T., Suzuki, K. (2004) Development of a new radioligand, *N*-(5-fluoro-2-phenoxyphenyl)-*N*-(2-[^{18}F]fluoroethyl-5methoxybenzyl)acetamide, for PET imaging of peripheral benzodiazepine receptor in primate brain. *J. Med. Chem.* 47, 2228-2235.

[70] Lin, K.-S., Ding, Y.-S., Kim, S.-W., Kil, K.-E. (2005). Synthesis, enantiomeric resolution, F-18 labeling and biodistribution of reboxetine analogs: promising radioligands for imaging the norepinephrine transporter with positron emission tomography. *Nucl. Med. Biol.* 32, 415-422.

[71] Zhang, M.-R., Maeda, J., Ito, T., Okauchi, T., Ogawa, M., Noguchi, J., Suhara, T., Halldin, C., Suzuki, K. (2005). Synthesis and evaluation of *N*-(5-fluoro-2-phenoxyphenyl)-*N*-(2-[^{18}F]fluoromethoxy-d_2-5-methoxybenzyl)acetamide: a deuterium-substituted radioligand for peripheral benzodiazepine receptor. *Bioorg. Med. Chem.* 13, 1811-1818.

[72] Tsukada, H., Sato, K., Fukumoto, D., Kakiuchi, T. (2006) Evaluation of D-isomers of *O*-^{18}F-fluoromethyl, *O*-^{18}F-fluoroethyl, and *O*-^{18}F-fluoropropyl tyrosine as tumor imaging agents in mice. *Eur. J. Nucl. Med. Mol. Imaging.* 33(9), 1017-1024.

[73] Chi, DY, Kilbourn, M.R., Katzenellenbogen, J.A., Welch. M.J. (1987) A rapid and efficient method for the fluoroalkylation of amines and amides. Development of a method suitable for incorporation of the short-lived positron emitting radionuclide fluorine-18. *J. Org. Chem.* 52, 658-664.

Vita

KERRY A. RIFFEL

1518 Liberty Bell Drive, Harleysville, PA, 215-361-0849, kerry_riffel@merck.com

---

EDUCATION:

Lehigh University, Bethlehem, PA
Major: Chemistry, Ph.D. anticipated 2006
GPA: 3.27

Washington State University, Richland, WA,
M.S. Environmental Science, December 1996
GPA: 3.78

Loyola College, Baltimore, MD
B.S. Chemistry, May 1994

PROFESSIONAL EXPERIENCE:

Merck & Co. Inc., Imaging Research
Research Chemist, April 2004 – Present

- Provide analytical support during the development of novel PET and SPECT tracers.
- Perform *in vitro* metabolism studies on novel PET tracers to evaluate stability in animal species vs. human using HPLC with radiochemical detection. Use LC-MS/MS for identification of metabolites.
- Perform analysis of metabolites from *in vivo* animal plasma samples for radiolabeled species using HPLC and radiochemical detection. Determine metabolite-corrected SUVs for PET tracers *in vivo* in plasma and whole blood samples from animal species.
- Develop and validate methods for the determination of drug concentrations in plasma from various animal species using liquid-liquid extraction and LC-MS/MS.
- Evaluate novel PET tracers for the presence of small amounts of impurities using LC-MS/MS, including identification of impurities.

Merck & Co. Inc., Clinical Drug Metabolism
Research Chemist, October 2000 – April 2004
Staff Chemist, July 1997 – October 2000

- Provide bioanalytical support for Merck drug development programs entering human clinical trials.
- Develop and validate analytical methods for drugs and/or their metabolites in human fluids using HPLC, LC-MS/MS, automated liquid-liquid and/or solid phase extraction.
- Prepare protocols and reports for completed projects.

- Contributed to the Drug Metabolism Safety Committee as follows: Vice-Chairperson in 2001 and Chairperson in 2002. Responsibilities included disseminating safety-related information to the department, chairing monthly committee meetings and participating on the MRL Safety Committee.
- Member of the Watson ClinLIMS committee: validation of software for 21CFR Part 11 compliance, assisted with training during the implementation of Phase II (analytical), backup to the Protocol Entry Specialist.
- Recruited for new-hires and interns for Drug Metabolism at Lehigh University, University of Maryland, Bryn Mawr College and Haverford College.

Washington State University, Department of Environmental Science, Food and Environmental Quality Laboratory
Research Assistant, June 1995-December 1996

- LC-MS analysis of sulfonylurea herbicides in environmental samples including atmospheric deposition, river water, and cherry and grape leaves.
- Performed maintenance on the LC-MS system and trained personnel on its use.
- Maintain compliance with EPA GLP guidelines.

Ocean Spray
Research Technician, Summers 1992-1994

- Conducted studies on cranberry plant nutrient uptake using ionic flow analysis and atomic absorption spectroscopy.
- Coordinated the collection of field samples according to study protocols.
- After departure of full-time technician, trained the new technician in the use and maintenance of laboratory equipment.

SOCIETY MEMBERSHIPS:

American Chemical Society; Agrochemical Division, Analytical Division

ACADEMIC AND PROFESSIONAL HONORS:

Merck Award for Excellence for contributions to the CCR2 clinical program, 12/2003
Merck Award for Excellence for contributions to the Simvastatin/Ezetimibe Bioequivalence study, 1/2003
Safety Begins Here Award for contributions to the Drug Metabolism Safety Committee, 12/2002
Merck Award for Excellence for contributions to Losartan pediatric filing, 1/2002
Merck Award for Excellence for contributions to PPAR clinical program, 10/2001
Honorable Mention for poster presentation at the Boeing Environmental Symposium,

Washington State University, April 1996
Dean of Students Recognition Luncheon, Loyola College, 1994
Student Leader, Spring Break Outreach, Loyola College, 1994
Invitation to attend the Emerging Women Leaders Conference, Loyola College, 1994
Baltimore Chemical Society scholarship for academic excellence, 1993

PUBLICATIONS:

Groff, M., Riffel, K.A., Song, H.H., Lo, M.-W. Stabilization and determination of a PPAR agonist in human urine using automated 96-well liquid-liquid extraction and liquid chromatography/tandem mass spectrometry. *J. Chrom. B.*, 842(2), 122-130, 2006.

Decochez, K., Rippley, R.R., Miller, J.L., De Smet, M., Yan, K.X., Matthuks, Z., Riffel, K.A., Song, H., Zhu, H., Maynor, H.O., Tanaka, W., Johnson-Levonas, A.O., Davies, M.J., Gottesdiener, K.M., Keymeulen, B., Wagner, J.A. A dual PPAR α/γ agonist increases adiponectin and improves plasma lipid profiles in healthy subjects. *Drugs RD.* 7, 99-110, 2006.

Migoya, E.M., Bergman, A.J., Hreniuk, D., Matthews, N., Yi, B., Roadcap, B.A., Valesky, R.J., Liu, L., Riffel, K.A., Groff, M., Zhao, J.J., Gamble, J.J., Kosoglou, T., Statkevich, P., Lasseter, K.C., Levonas, A., Murphy, M.G., Gottesdiener, K.M., Paolini, J.F. Bioequivalence of the ezetimibe/simvastatin combination tablet and co-administration of ezetimibe and simvastatin as separate tablets in healthy subjects. *Int. J. Clin Pharm. Ther.* 44, 83-92, 2006.

Hamill, T.G., Krause, S., Ryan, C., Bonnefous, C., Govek, S., Seiders, T.J., Cosford, N.D.P., Roppe, J., Kamenecka, T., Patel, S., Gibson, R.E., Sanabria, S., Riffel, K., Eng, W., King, C., Yang, X., Green, M.D., O'Malley, S.S., Hargreaves, R., Burns, H.D. Synthesis, characterization, and first successful monkey imaging studies of metabotropic glutamate receptor subtype 5 (mGluR5) PET radiotracers. *Synapse*, 56, 205-216, 2005.

Riffel, K.A., Groff, M.A., Wenning, L., Song, H., Lo, M.-W. Fully automated liquid-liquid extraction of a novel insulin sensitizer in human plasma by heated nebulizer and turbo ionspray liquid chromatography-tandem mass spectrometry. *J. Chrom. B.*, 819, 293-300, 2005.

Riffel, K., Polinko, M., Song, H., Rippley, R., Lo, M.W. Quantitative determination of a novel insulin sensitizer and its para-hydroxylated metabolite in human plasma by LC-MS/MS. *J. Pharm. Biomed. Anal.*, 35 523-534, 2004.

Polinko, M., Riffel, K., Song, H., Lo, M-W. Simultaneous determination of losartan and EXP3174 in human plasma and urine utilizing liquid chromatography/tandem mass spectrometry. *J. Pharm. Biomed. Anal.* 33:73-84, 2003

Yan, K., Song, H., Riffel, K., Lo, M-W. Simultaneous determination of a novel M_3 muscarinic receptor antagonist and its 5-OH metabolite in human plasma using liquid chromatography/tandem mass spectrometry. *J. Pharm. Biomed. Anal.* 27: 699-709, 2002.

Song, H., Gu, X., Riffel, K., Yan, K. and Lo, M-W. Determination of a novel thrombin inhibitor in human plasma and urine utilizing liquid chromatography with tandem mass spectrometric and ultraviolet detection. *J. Chromatogr. B*, 738: 83-91, 2000.

Riffel, K.A., Song, H., Gu, X., Yan, K. and Lo, M-W. Simultaneous determination of a novel thrombin inhibitor and its two metabolites in human plasma by liquid chromatography/tandem mass spectrometry. *J. Pharm. Biomed. Anal.* 23: 607-616, 2000.

Davenport, J.R., Carpenter, J. and Sullivan, K. Multiple year fruiting in cranberries in New Jersey. *Cranberries* 59 (5): 10-11, 1995.

ABSTRACTS:

Riffel, K.A., Hamill, T.G., Hostetler, E.D. Burns, H.D. Use of LC-MS/MS for the Evaluation of the Presence of Impurities in Two Novel PET Tracers. *American Society of Mass Spectrometry* Annual Meeting, Seattle, WA, May 2006.

Riffel, K., Polinko, M., Song, H., Lo, M.W. Quantitative Determination of a Novel Insulin Sensitizer and its Para-Hydroxylated Metabolite in Human Plasma by LC-MS/MS. American Chemical Society Annual Meeting, Boston, MA, August 2002.

Polinko, M., Riffel, K.A., Song, H., and Lo, M-W. Simultaneous Determination of losartan and EXP3174 in human plasma and urine utilizing liquid chromatography/tandem mass spectrometry. *American Chemical Society*, Orlando, FL, April 2002.

Riffel, K., Song, H., Gu, X., Yan, K. and Lo M.-W. Simultaneous determination of L-375,378, a potent orally active thrombin inhibitor, and its two metabolites in human plasma by LC-MS/MS. *AAPS PharmSci Supplement* 1 (4): S-302, 1999.

Sullivan, K.A. and Weisskopf, C.P. The analysis of Sulfonylurea Herbicides Using High Performance Liquid Chromatography-Mass Spectrometry. *American Chemical Society* Annual Meeting, Orlando, Florida, August 1996.

Felsot, A.S., Bhatti, M.A., Sullivan, K.A. and Weisskopf, C.P. Are Airborne Herbicide Residues Hazardous to Nontarget Crops? *American Association for the Advancement of Science*, Pacific Division Annual Meeting, San Jose, California, June 1996.

Sullivan, K.A. and Weisskopf, C.P. The Analysis of Sulfonylurea Herbicides Using High Performance Liquid Chromatography-Mass Spectrometry. *Boeing Environmental Symposium*, Pullman, Washington, April 1996.

Davenport, J.R., Broaddus, A., Fitzpatrick, S., Provost, J. and Sullivan, K. Do cranberries take up nutrients during the "dormant season"? *Proceedings of the 1993 North American Cranberry Research and Extension Workers Conference*, 1993.

Davenport, J.R., Provost, J. and Sullivan, K. Chlorophyll meters as a tool to monitor cranberry nitrogen needs. *Proceedings of the 1993 North American Cranberry Research and Extension Workers Conference*, 1993.